

1 This paper is a non-peer reviewed preprint submitted to EarthArXiv

2  
3 **Reframing Lake Geneva ecological trajectory in a context of multiple but asynchronous**  
4 **drivers**

5  
6 **Rosalie Bruel** <sup>(1, 2)\*</sup>, **Stéphanie Girardclos** <sup>(3, 4)</sup>, **Aldo Marchetto** <sup>(5)</sup>, **Katrina Kremer** <sup>(3, 6)</sup>,  
7 **Christian Crouzet** <sup>(7)</sup>, **Jean-Louis Reyss** <sup>(8)</sup>, **Pierre Sabatier** <sup>(8)</sup>, **Marie-Elodie Perga** <sup>(1, 9)</sup>

8 (1) CARRTEL, INRA, Université Savoie-Mont Blanc, 74200 Thonon-les-Bains, France

9 (2) Rubenstein Ecosystem Science Laboratory, University of Vermont, 05401 Burlington VT, US

10 (3) Dept of Earth Sciences, University of Geneva, Rue des Maraîchers 13, CH-1205 Geneva, Switzerland

11 (4) Institut des Sciences de l'Environnement (ISE), University of Geneva, Boulevard Carl Vogt 66, CH-  
12 1205 Geneva, Switzerland

13 (5) CNR-IRSA, Largo Tonolli 50, 28922 Verbania Pallanza, Italy

14 (6) present address: Swiss Seismological Service, ETH Zurich, Sonneggstrasse 5, 8092 Zurich, Switzerland

15 (7) Univ. Grenoble Alpes, Univ. Savoie Mont Blanc, CNRS, IRD, IFSTTAR, ISTerre, 38000 Grenoble,  
16 France

17 (8) EDYTEM, Université Savoie-Mont Blanc, CNRS, 73370, Le Bourget du Lac, France

18 (9) IDYST, Université de Lausanne, Mouline, 1015 Lausanne, Switzerland

19 \*Corresponding author

20 **Authors email.**

- 21 - RB [rosaliebruel@gmail.com](mailto:rosaliebruel@gmail.com)  
22 - SG [Stephanie.Girardclos@unige.ch](mailto:Stephanie.Girardclos@unige.ch)  
23 - AM [aldo.marchetto@cnr.it](mailto:aldo.marchetto@cnr.it)  
24 - KK [katrina.kremer@sed.ethz.ch](mailto:katrina.kremer@sed.ethz.ch)  
25 - CC [Christian.Crouzet@univ-smb.fr](mailto:Christian.Crouzet@univ-smb.fr)  
26 - JLR [Jean-Louis.Reyss@univ-smb.fr](mailto:Jean-Louis.Reyss@univ-smb.fr)  
27 - PS [Pierre.Sabatier@univ-smb.fr](mailto:Pierre.Sabatier@univ-smb.fr)  
28 - MEP [marie-elodie.perga@unil.ch](mailto:marie-elodie.perga@unil.ch)  
29

30 **Keywords.** Resilience, climate warming, temporal ecology, paleoecology, lake, interactive carryover

31 **Type of article.** Research Article

32 **Running title.** Multiple asynchronous drivers of Lake Geneva trajectory

33 **7 figures, 0 table, 0 box**

34 **Materials & Correspondence.** Requests should be addressed to [rosaliebruel@gmail.com](mailto:rosaliebruel@gmail.com) / Rubenstein  
35 Ecosystem Science Laboratory, 3 College St., Burlington, VT 05401, USA

36 **Abstract**

37 **There are no doubts long-term observatories provide unique insight on ecosystems**  
38 **trajectories. Can we use earliest data to set restoration goals? We take the example of Lake**  
39 **Geneva, for which descriptions of the ecosystem are available for as soon as the late 19<sup>th</sup> and**  
40 **early 20<sup>th</sup> century. Forel writes about how the luxuriant growth of plant communities provided**  
41 **important habitat for aquatic animals, as well as trapping nutrients and affecting water**  
42 **currents. It can be hard to believe Forel is referring to the same lake as present-day Lake**  
43 **Geneva; however, without continuous monitoring, this qualitative description can hardly be**  
44 **compared to recent observations. We resorted to paleolimnology to quantify the changes in**  
45 **plankton communities, as a proxy of general ecological changes, over the past 1,500 years. Our**  
46 **results show that from 563 AD (beginning of the record) to the 20<sup>th</sup> century, the cladoceran**  
47 **assemblage remained stable, despite important amplitude of climate variability (3°C).**  
48 **Trajectory of Lake Geneva shifted for the first time in 1946. Online dynamic linear models**  
49 **revealed the following transition, in 1958-1961, transition was critical, i.e., the ecosystem**  
50 **changed state. Littoral associated species were totally lost, and the assemblage is now**  
51 **dominated by pelagic species. The shift took place around the beginning of the long-term**  
52 **monitoring program, when local perturbations (eutrophication) were escalating. Our result**  
53 **raises the vexing observation that the historical dataset, one of the longest records in the world,**  
54 **may not provide a baseline for Lake Geneva's condition.**

55

## 56 **Introduction**

57 There is no specific data crisis for Lake Geneva (CH, FR). It is one of the lakes in the world with  
58 the largest amount of data, going back to the end of the 19<sup>th</sup> century (Forel 1892), and with a regular  
59 monitoring since 1957 (SOERE OLA-IS). In the early stages of the monitoring, managers recorded  
60 the increase of total phosphorus (TP) going from 10  $\mu\text{g P.l}^{-1}$  (i.e., close to background levels,  
61 inferred at 6-8  $\mu\text{g.l}^{-1}$  from diatoms, Berthon et al. 2013) to 50  $\mu\text{g P.l}^{-1}$  in the early 1960s, and up to  
62 90  $\mu\text{g P.l}^{-1}$  in the late 1970s.

63 The long-term monitoring is expected to have captured the major and dominant modifications in  
64 Lake Geneva ecology because the record began at the heel of the “hockey stick curve” of human  
65 pressures on Lake Geneva (Alric et al. 2013; Jenny et al. 2014). Both old records and recent findings  
66 yet cast doubts on this assumption. Detailed observations by the pioneer limnologist FA Forel at the  
67 very beginning of the 20<sup>th</sup> century reported thriving macrophytic, charophytic belts around the lake  
68 in 1904, forming “true underwater forests, as picturesque, mysterious and attractive as the most  
69 beautiful forests of your mountains” (translation by Vincent and Bertola 2014), a feature which let  
70 no traces in the 1975, 1997, and 2009 macrophyte surveys (Perfetta 2011).

71 Initial evaluations, using correlation between TP and phytoplankton biomass, established that levels  
72 around 20  $\mu\text{g P.l}^{-1}$  would allow restoration of Lake Geneva (CIPEL 2007). Eutrophication was  
73 tackled by the effort of Swiss (first) and French (later) politics from the late 1970s. The 20  $\mu\text{g P.l}^{-1}$   
74 were reached, a decade ago, without any quantifiable decline in algal biomass or production. In the  
75 meanwhile, evidence that other anthropogenic drivers were at play in promoting algal growth had  
76 been produced (Tadonl  k   et al. 2009; Alric et al. 2013). Thereafter, the restoration goal was  
77 reviewed to target 10-15  $\mu\text{g P.l}^{-1}$  (CIPEL 2010), to account for potential additive or synergistic  
78 effect of nutrient enrichment with other human pressures. This concentration range actually  
79 corresponds to the earliest phosphorous concentrations ever measured in the lake, at the beginning  
80 of the monitoring survey in the late 1950s (Berthon et al. 2013). Although phosphorus levels are  
81 asymptotically reaching this second target, both primary production and algal biomass are still  
82 comparable to those of maximum eutrophication (CIPEL 2018, pp. 106–112).

83 Explaining the decoupling between initial driver and symptom of eutrophication requires to  
84 remember that ecosystems are the complex output of both space and time constraints (Wolkovich  
85 et al. 2014). Relative stability is guaranteed by feedback mechanisms (endogenous processes),  
86 conferring them resilience towards exogenous perturbation (Hodgson et al. 2015). When exogenous

87 drivers exceed endogenous feedbacks, systems can shift to an alternative state (Scheffer and  
88 Carpenter 2003). The presence of multiple drivers is rather the norm, but the increase of  
89 anthropogenic pressure since the 19<sup>th</sup> century is pushing many ecosystems close to their limits of  
90 resistance, to an alternative state (Rocha et al. 2015). The possibility for critical transitions even in  
91 large lakes is now being reconsidered under the hypothesis that they may occur at even lower  
92 nutrient thresholds in large and deep lakes than in shallow lakes (Hilt et al. 2010; Hilt 2015; Bruel  
93 et al. 2018). Regime shifts come along with major reorganization of ecological processes, creating  
94 a whole new set of mechanisms ruling the new ecological regime (Carpenter 2005). Such  
95 rearrangements then affect how and how much the system respond to the initial driver (accumulative  
96 carryover), but also to external drivers other than the one that created the shift (interactive carryover,  
97 Ryo et al. 2019). An ecosystem that shifted can be vulnerable to further shifts through dominos  
98 effect or hidden feedback mechanisms (Rocha et al. 2018).

99 If Lake Geneva actually shifted early to an alternative state, not only the lake we currently monitor  
100 would be different in biological composition to the one that fascinated Forel, but it would also differ  
101 in the way its biology responds to other drivers, such as climate variability. So, was Forel's Lake  
102 Geneva the same lake that we have been monitoring so far? Or in contrast, had the lake already  
103 significantly changed in ecological state before the monitoring started? Did Lake Geneva actually  
104 experience a regime shift already before being under surveillance? The questions of patterns and  
105 scales are crucial in ecology (Levin 1992); our primary objective is to reframe the long-term  
106 monitoring data in a longer perspective. Our second objective is to formulate hypotheses on  
107 implications of an alternative new state when it comes to establish restoration goals.

108 We resort to paleoecology, to extend beyond the instrumental monitoring records and cover for the  
109 last 1.5 millenniums. Paleoecology gives the possibility to cover long period of times on a single  
110 system, allowing to get rid of the variations linked to geographical area and different local settings.  
111 Biological proxies (diatoms and cladocerans) were retrieved and analyzed from an accurately dated  
112 composite sediment core. Sub-fossil diatom records were used to infer past concentrations in total  
113 phosphorous (Wunsam and Schmidt 1995), while sub-fossil cladocerans were regarded as the proxy  
114 for ecological responses, as they show high sensitivity to changes in the environment, recording  
115 bottom-up changes in resources, alterations in habitat structure, and diversity and top-down impacts  
116 of predation (Davidson et al. 2011). First, we used multivariate analyses to visualize the trajectory  
117 of Lake Geneva cladoceran assemblage. Paleorecords can be characterized by differences in  
118 compaction and mixing, that can impact detection of changepoint by traditional methods (Taranu et  
119 al. 2018). As a result, we turned to online dynamic linear models to assess whether any transition

120 was critical (Taranu et al. 2018). We used General Additive Models to identify the contribution of  
121 local versus climate drivers (Wood 2016). We resort to paleoecology, to extend beyond the  
122 instrumental monitoring records and cover for the last 1.5 millennium. Paleoecology gives the  
123 possibility to cover long period of times on a single system, allowing to get rid of the variations  
124 linked to geographical area and different local settings. Biological proxies (diatoms and  
125 cladocerans) were retrieved and analyzed from an accurately dated composite sediment core. Sub-  
126 fossil diatom records were used to infer past concentrations in total phosphorous (Wunsam and  
127 Schmidt 1995), while sub-fossil cladocerans were regarded as the proxy for ecological responses,  
128 as they show high sensitivity to changes in the environment, recording bottom-up changes in  
129 resources, alterations in habitat structure, and diversity and top-down impacts of predation  
130 (Davidson et al. 2011). First, we used multivariate analyses to visualize the trajectory of Lake  
131 Geneva cladoceran assemblage. Paleorecords can be characterized by differences in compaction and  
132 mixing, that can impact detection of changepoint by traditional methods (Taranu et al. 2018). As a  
133 result, we turned to online dynamic linear models to assess whether any transition was critical  
134 (Taranu et al. 2018). We used General Additive Models to identify the contribution of local versus  
135 climate drivers (Wood 2016).

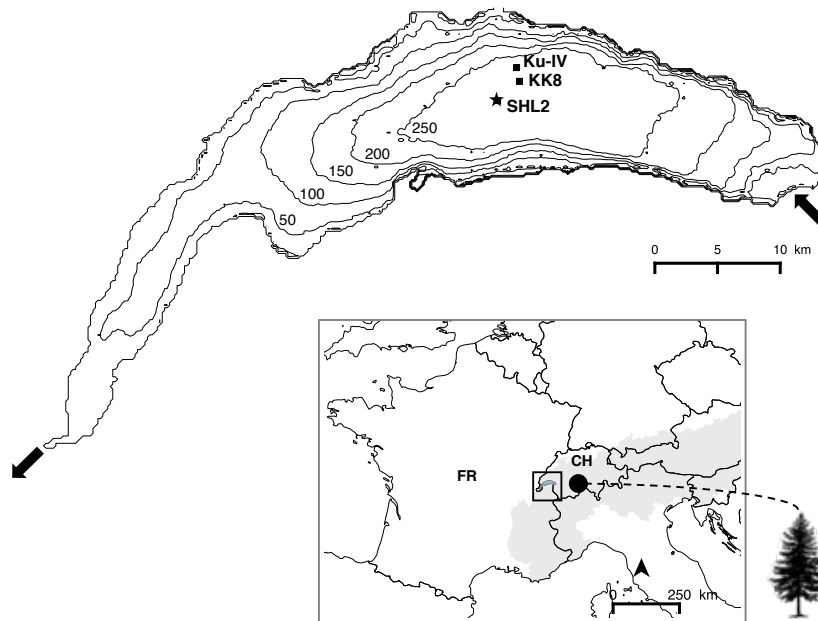
136

## 137 **Materials and methods**

### 138 *Study site*

139 Lake Geneva is the largest lake of Western Europe, with a maximum depth of 309 meters (Fig.  
140 1\_MAP). The human population in its watershed has increased threefold since the late 19<sup>th</sup> century,  
141 directly initiating the well documented eutrophication. Observed concentration in Lake Geneva has  
142 been below 20  $\mu\text{g P}\cdot\text{l}^{-1}$  since the 2010s. Although Lake Geneva's hydrological function had been  
143 impacted since the first dam was built in the late 19<sup>th</sup> century at the lake outflow, it is the changes  
144 in TP that have triggered the onset of deep water hypoxia (Jenny et al. 2014) as well as quantitative  
145 and qualitative changes in planktonic (Anneville and Pelletier 2000; Alric et al. 2013; Berthon et al.  
146 2014) and fish (Anneville et al. 2017) populations since the 1950s. At the same time, the regional  
147 atmospheric warming has reached +2°C over the 20<sup>th</sup> century, i.e., twice the global average, with a  
148 first warming phase starting in the 1930s and 1940s. Evidence suggests that the most recent  
149 atmospheric warming (since the 1980s), superimposed on fluctuations in TP, has altered the

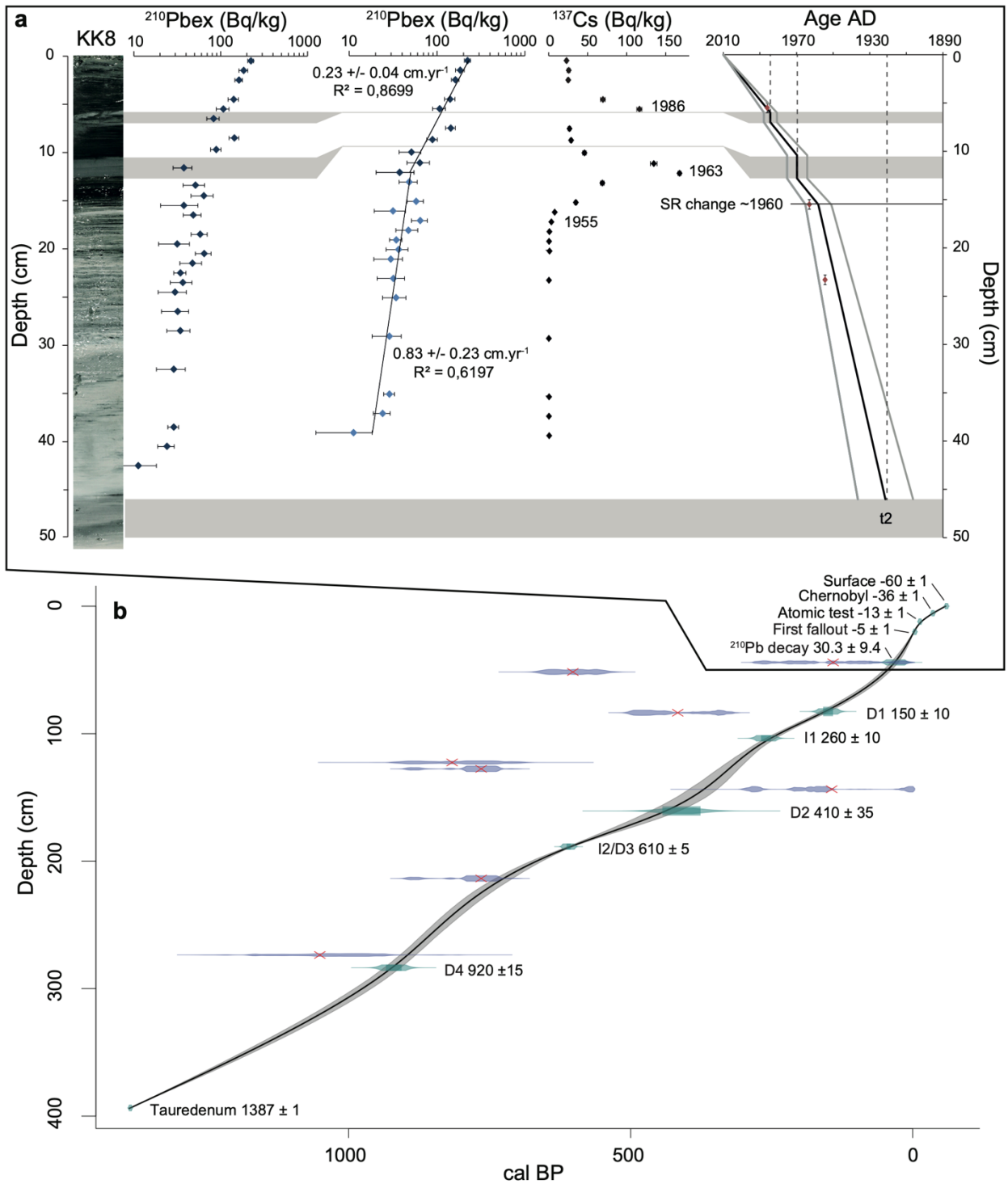
150 physical, biogeochemical, and ecological structure of Lake Geneva (Alric et al. 2013; Perga et al.  
151 2015; Anneville et al. 2017).



152  
153 **Figure 1\_MAP.** Lake Geneva lies at the border between France (FR) and Switzerland (CH) in the  
154 peri-alpine domain (Alps as grey surface on the bottom-right insert map). The bathymetry (in  
155 meters), sediment core localization (black squares), and monitoring point (star) are indicated.  
156 Arrows indicate the Rhône river inflow and outflow. The black circle on the bottom insert map  
157 shows the location of the four trees-ring sites used by Büntgen et al. (2006) to reconstruct SAT  
158 anomalies.

159  
160 *Sediment record and dating*

161 A paleo-record dataset was built using two sediment cores collected in 2010 in the deepest basin of  
162 Lake Geneva. The two closely spaced sediment records were merged into one composite record  
163 LEM10-CC using the stratigraphic level of turbidite t2 as identified by Kremer et al. (2015). Dating  
164 relied on radionuclide measurements for the upper part of the core, previous <sup>14</sup>C measurements  
165 (Kremer et al. 2012), and new paleomagnetic secular variations measurements for the deeper section  
166 (Fig. 2\_AGEMODEL). Details are given in Supplementary Materials S1.



167

168 **Figure 2\_AGEMODEL. a)** Chronology (with  $1\sigma$  uncertainties) of the uppermost part of core KK8  
 169 based on activity of short-lived radionuclides ( $^{210}\text{Pbex}$  and  $^{137}\text{Cs}$ ) and the application of a CFCS  
 170 model to the event-free sedimentary profile of  $^{210}\text{Pbex}$  (right panel). Uncertainties of  $^{137}\text{Cs}$  activities  
 171 are included as dots size. A main sedimentation rate (SR) change appears around 1960 AD. Grey  
 172 bands correspond to event layers / turbidite intervals, interpreted as instantaneous deposits  
 173 (relatively to the rest of the chronology). **b)** Age-depth model of composite record LEM10-CC built

174 with Clam R-code package (Blaauw 2010a) from 11 stratigraphic horizons. Event layers with  
175 thickness above 1 cm were interpreted as instantaneous events (Kremer et al. 2015) and removed  
176 before the age model computation. The envelope (grey area) represents the 2-sigma probability  
177 interval. Data not used to fit the age model ( $^{14}\text{C}$  dating) are marked with a red cross. See  
178 Supplementary Materials S1 for details.

179

### 180 *Selection of climate data*

181 Lack of restoration in Lake Geneva could be explained by recent climate change (Alric et al. 2013).  
182 We seek long-term air temperature records to establish whether similar warming episodes took  
183 place. A substantial climatic variability has been reported for the past 1,500 years in central Europe.  
184 A notably cold period was likely triggered by a volcanic eruption in the “Dark Age”, 536–660 AD  
185 (Larsen et al. 2008; Büntgen et al. 2016), followed by a prolonged period of relative climate stability  
186 (Medieval Quiet Period, ~725–1025 AD, Bradley et al. 2016). The ensuing Medieval Warm Period  
187 (MWP, ca. 900–1300 AD) showed average summer air temperatures (SAT) similar to those  
188 observed between the 1950s and 1970s ( $0^\circ\text{C}$  SAT anomaly, Ljungqvist 2010). There then followed  
189 a new cold period, the LIA (ca. 1300–1850 AD;  $-3^\circ\text{C}$  SAT anomaly, Ljungqvist 2010) before the  
190 recent warming (recent Climate Change rCC, 1850-present, Abram et al. 2016), mainly attributed  
191 to human impact.

192 Climate fluctuations over the past millennia are marked by significant regional offsets (Crowley and  
193 Lowery 2000; Mann and Jones 2003). It was thus essential to choose a relevant reconstruction of  
194 the climatic forcing, but also to understand the region it accounts for, as some climatic signals are  
195 more regional than others. We selected a local reconstruction of SAT anomalies from the Rhône  
196 valley, directly linked to Lake Geneva (Büntgen et al. 2006). The record goes back to 755 AD,  
197 corresponding to the last 1,250 years of our sediment record. When cladoceran sample covered  
198 several years, an average SAT anomaly was calculated for the same period and used to provide the  
199 climatic context for Lake Geneva.

200

### 201 *Reconstruction of TP levels*

202 In Lake Geneva, a long-term monitoring program, initiated in 1958, spans most of the eutrophication  
203 and the re-oligotrophication phases. Changes in total phosphorus concentrations were inferred from

204 diatom sub-fossil remains for the previous period when there was no monitoring data  
205 (Supplementary Materials S2). We used a composite TP record (DI-TP until 1957, monitoring data  
206 from 1958), thereafter referred to as I-TP. The confidence in I-TP is very high as the first changes  
207 in diatoms communities took place after the onset of the monitoring program.

208

### 209 *Ecological dynamic*

210 Cladocera were regarded as the main proxy for ecosystem state. Continuous sub-sampling of  
211 LEM10-CC was carried out, and one out of three samples were selected for cladoceran remains  
212 counting. Remains were analyzed according to Frey (1986): a minimum number of 400 cladoceran  
213 remains per sample (headshields, shells, post-abdomens, post-abdominal claws, mandibles and  
214 others) were counted and identified using the determination keys of Szeroczynska and Sarmaja-  
215 Korjonen (2007) and an Olympus BX41 microscope at 100-200 magnification. *Bosmina* sp. were  
216 determined to the species level (*B. longirostris*, *E. longispina*, and *E. coregoni*), as well as  
217 chydorids, whenever possible. Regarding the complexity of the taxa (Alric et al. 2016), *Daphnia*  
218 spp. were identified to the genus level.

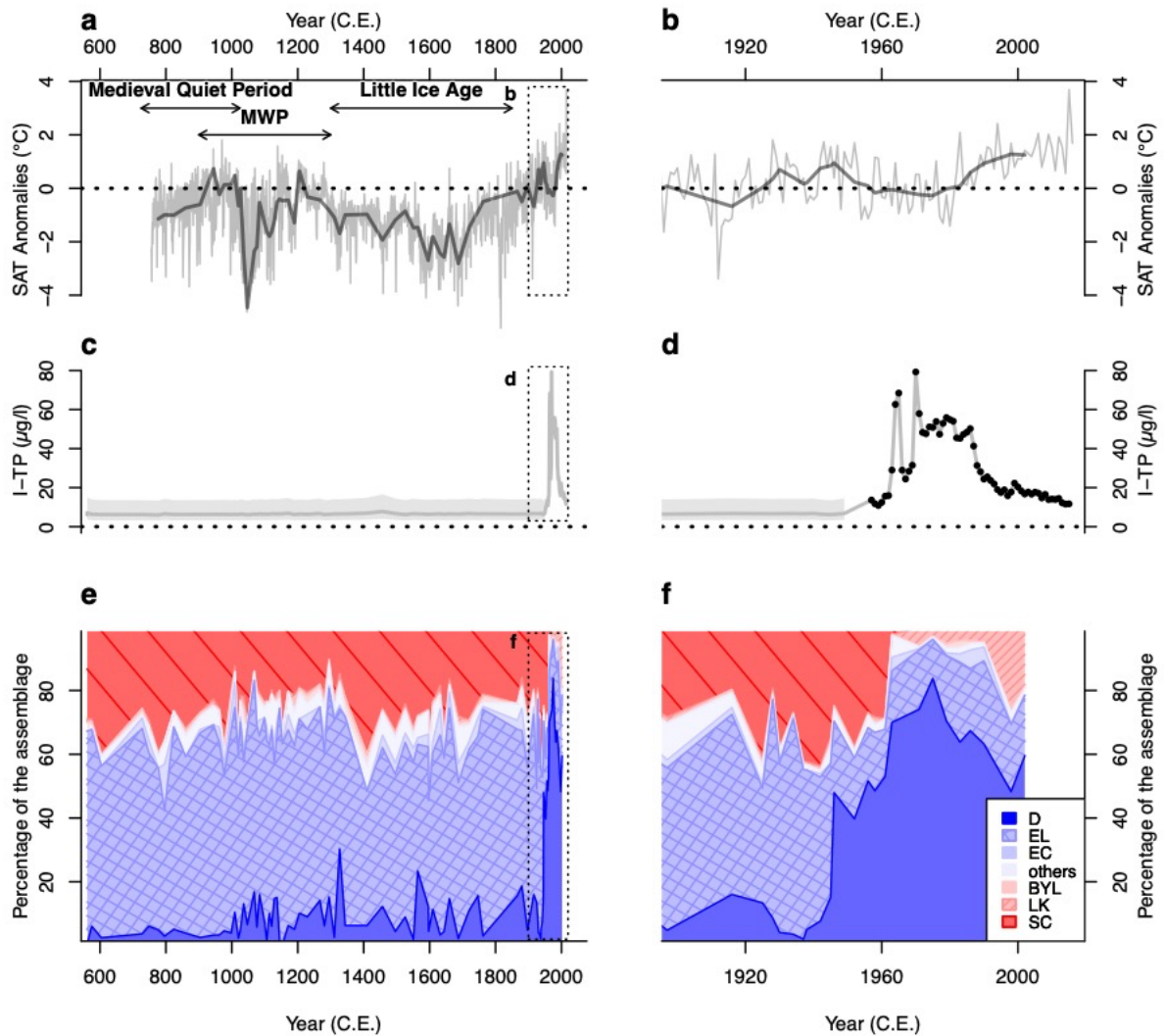
219

### 220 *Statistical analysis*

221 The main dynamics of the cladoceran community over time were summarized using Principal  
222 Component Analysis (PCA, an indirect gradient analysis method, Jolliffe 1986), after Hellinger  
223 transformation of the percent data. We then turned to online dynamic linear models (DLMs, Pole et  
224 al. 1994) to evaluate whether any transition had the characteristics of critical transitions (method in  
225 Taranu et al. 2018). Shortly, DLMs are used to model and forecast in time-series analysis. The  
226 modelling part of DLMs strongly borrows from the regression model family, while the forecasting  
227 resembles the ARIMA models logic. While in a linear regression model, parameters are statics, in  
228 DLMs, parameters are treated as time-varying. DLMs will proceed to estimate state at time  $t$ , using  
229 all observations since the beginning of the time-series up to  $t-1$ , and tolerating lags ( $p$  in  $AR(p)$ ).  
230 The method we used is well suited to long-term paleo-reconstructions because it handles missing  
231 values in the time series (Copyright 2017, Stephen R. Carpenter, method published in Taranu et al.  
232 2018). A critical transition is characterized by eigenvalues of the Jacobian matrix crossing 1 from  
233 below, indicating the system lost its capacity of returning toward the mean (i.e., its previous state:

234 the system goes into a new state. Scheffer et al. 2015b). Best lag and delta (discount factor,  
 235 accounting for variance) were chosen by computing AIC scores.

236



237

238 **Figure 3\_DESCRIPTIF.** Changes in temperature, lake phosphorus concentrations, and cladocera  
 239 assemblage since 563 AD. (a, b) Reconstructed summer (June to August) air temperature anomaly  
 240 (SAT anomaly) from the Rhone valley (Switzerland) for the 755–1960 time period. Measured SAT  
 241 converted into SAT anomaly at the Cointrin weather station (Switzerland) for the 563–2016 (a) and  
 242 1900–2016 (b) time-interval. Light grey line represents annual data; dark grey line represents the  
 243 selected temperature for each sample, accounting for changes in sample thickness and sedimentation  
 244 rate. (c, d) Diatom-inferred total phosphorus (DI-TP) concentration (thick grey line, with confidence  
 245 interval) compared to the monitoring data for the 563–2016 (c) and 1900–2016 (d) time-interval  
 246 (SOERE SI-OLA, Thonon-les-bains, France). (e, f) Changes in cladoceran assemblage for the 563–

247 2016 (e) and 1900–2016 (f) time-interval. D: *Daphnia* spp., EL: *Eubosmina longispina*, EC:  
248 *Eubosmina coregoni*, BYL: *Bythotrephes longimanus*, LK: *Leptodora kindtii*, SC: *Sida crystallina*,  
249 others: other taxa.

250

## 251 **Results**

### 252 *Age model*

253 The excess  $^{210}\text{Pb}$  profile measured on core KK8 showed a regular decrease punctuated by two drops  
254 in  $^{210}\text{Pb}_{\text{ex}}$  on the profile (Fig. 2\_AGEMODEL\_a). Following the lithology and Arnaud et al. (2002),  
255 these low values of  $^{210}\text{Pb}_{\text{ex}}$  refer to instantaneous deposits and thus were excluded from the  
256 construction of the event-free sedimentary record.  $^{210}\text{Pb}_{\text{ex}}$  activities plotted on a logarithmic scale  
257 revealed two different mean sedimentation rates (SR), respectively of  $0.23 \pm 0.04 \text{ cm.yr}^{-1}$  above  
258 12.1 cm (event-free sequence) and  $0.83 \pm 0.23 \text{ mm.yr}^{-1}$  below this depth. Ages of the original  
259 sediment sequence provide a continuous age-depth relationship with a main sedimentation change  
260 dated around 1960 AD and  $1919.7 \pm 9.4 \text{ AD}$  for the event layer t2 (turbidite). The  $^{137}\text{Cs}$  activity  
261 profile reveals two peaks at  $5.5 \text{ cm} \pm 5 \text{ mm}$  and  $15.5 \text{ cm} \pm 5 \text{ mm}$ , corresponding respectively to  
262 1986 (Chernobyl accident) and 1963 (atmospheric atomic tests) (Appleby et al. 1991). Below  $23.5$   
263  $\text{cm} \pm 5 \text{ mm}$ , the recorded  $^{137}\text{Cs}$  activities are close to zero, pointing to a sequence deposited before  
264 1955 (first  $^{137}\text{Cs}$  fallout). These three  $^{137}\text{Cs}$  markers are in good agreement with the CFCS age model  
265 over the last century which confirms its reliability (Fig. 2\_AGEMODEL\_a).

266

267 From the event free composite core LEM10-CC, we calculated a continuous age-depth relationship  
268 with the R-code package ‘Clam’ version 2.2 (Blaauw 2010b). This age model integrates 11  
269 stratigraphic horizons (Supplementary Materials S1, Table S1.2): i) the coring year, ii) three time-  
270 markers from  $^{137}\text{Cs}$  activity, iii) the age of turbidite t2 dated from  $^{210}\text{Pb}$  profile, iv) five dated points  
271 from the new paleomagnetic study (Crouzet et al. 2019), together with v) the 563 AD historical time  
272 marker. The chronology of the composite record LEM10-CC was already constrained on the 563-  
273 2010 time-period by the Tauredunum deposit event and the coring year. The new chronology adds  
274 data from short-lived radionuclide activities and paleomagnetic secular variations allowing a rare  
275 dating precision in regard to the length of the core. The best Clam model was obtained using a  
276 smooth spline interpolation with a smoothing term of 0.32 which avoids sudden change in

277 sedimentation rates (Fig. 2\_AGEMODELb). We also tested the age-depth model using the Bayesian  
278 model Bacon (Blaauw and Christen 2011) with the same input data (Supplementary Materials S1).  
279 This independent Bacon model allows a comparison with Clam model and shows that both curves  
280 have the same trend. The Clam model was favored because it better fits the original time markers  
281 of radionuclides markers that are important for a precise 20<sup>th</sup> century chronology.

282

### 283 *Total phosphorus levels as a proxy for local human impact*

284 The diatom fossil assemblage was dominated by *Pantocsekiella comensis*, a species typical of  
285 oligotrophic lakes (Harris 1987; Willen 1991; Hall and Smol 2010), over the whole period preceding  
286 the onset of the monitoring (Supplementary Materials S2). TP concentrations inferred from diatom  
287 assemblages confirm that no significant changes in I-TP were recorded for the period 563–1957 AD  
288 (Fig. 3\_DESCRIPTIFc&d) despite a long history of human presence in Alpine Europe (Kaplan et  
289 al. 2009).

290

### 291 *Ecological changes inferred from cladoceran assemblages*

292 Our results show that the “recent” cladoceran assemblage is radically different from the one  
293 characteristic of the 563–1940 period (Fig. 3\_DESCRIPTIFe&f). Major ecological changes were  
294 summarized by two primary principal components of the cladoceran assemblages (PC1 and PC2,  
295 Fig. 4\_PCA) of the ordination analysis that accounted for 80% of the total variability within the  
296 dataset.

297 The excellent coherence of the signal recorded on the partial overlapping zones of the two cores  
298 with the previously published record of Alric *et al.* (2013) attests for the reproducibility of our  
299 results for the pelagic zone of Lake Geneva. The species distribution was largely unbalanced, with  
300 6 species being dominant in the record (Fig. 4\_PCAs). For clarity purposes, we grouped the  
301 remaining species in a group “others”. These species are mainly littoral (macrophyte and/or  
302 sediment associated, Fig. 4\_PCAb).

303 From the beginning of the record and for twelve centuries, the cladoceran community of Lake  
304 Geneva was dominated by the same two species, the pelagic *Eubosmina longispina*, the earliest  
305 postglacial colonist in alpine lakes (Nauwerck 1991), and *Sida crystallina* var. *limnetica* (Fig.

306 3\_DESCRIPTIFe&f). The latter species occupies both pelagic and littoral habitats (Forel 1892),  
307 which supports the likely presence of macrophytic belts around the lake before the 20<sup>th</sup> century.  
308 From the 1940s, the absolute abundance of both *Daphnia* spp. and *S. crystallina* increased (Fig.  
309 3\_DESCRIPTIFd). This period likely marks a period during which the food elemental quality  
310 improved, benefiting to *Daphnia* spp. that has high stoichiometric requirements (Urabe et al. 1997;  
311 Elser et al. 2001; Hessen et al. 2002). Levels of phosphorus increased, but under a threshold that  
312 prevented any restructuring in the phytoplankton assemblage (Supplementary Materials S2,  
313 DeMott and Gulati 1999). Furthermore, the maintenance of *S. crystallina* followed by its decline  
314 hint that no changes in algal biomass took place in the <10 µgTP.L<sup>-1</sup> range, since the resulting light  
315 limitation would have compromised the maintenance of the macrophyte-associated specie. From  
316 the early 1960s, when concentration went beyond 10-20 µgTP.L<sup>-1</sup>, *Daphnia* spp. eliminated *E.*  
317 *longispina*, while the habitat-demanding *S. crystallina*, that had been continuously present since 563  
318 AD, almost vanished in Lake Geneva in 1961 AD. *Daphnia* spp. made the most of the nutrient  
319 driven changes in the phytoplankton community structure while the herbivorous *E. longispina* suffer  
320 from their lower feeding efficiency compared to the larger phytoplankters. Such successive  
321 transitions have been confidently attributed to eutrophication (GAM for PC1 including a significant  
322 smooth term for I-TP, Dev. Expl.= 79.4%, df= 4.077, F= 55.99, p = 2.78·10<sup>-37</sup>, Fig. 5\_GAM) (Alric  
323 et al. 2013), and occurred at a relatively low I-TP threshold of 10–20 µgP.L<sup>-1</sup>. Between 1946 and  
324 1961 AD, the pristine Lake Geneva, hosting both littoral and planktonic habitats, shifted to an  
325 anthropogenic impacted, plankton-dominated state.

326 The best DLM was obtained for a *lag* of 1 and a *delta* of 0.84, and gave a R<sup>2</sup> of 0.80, and indicates  
327 a transition in 1958/1961 (Fig. 6\_DLMc). Note that S. Carpenter (who coded the script)  
328 recommends *deltas* ranging from 0.9 to 0.99. Constraining DLM to that window resulted in a  
329 slightly lower fit (R<sup>2</sup>= 0.79 for *delta*= 0.9), but no change in critical transition (1958/1961). *Delta*  
330 accounts for potential variability in the time-series being tested for critical transition. Lower *delta*  
331 is smoothing the signal, which explains the inverse relationship between R<sup>2</sup> and *delta*. The DLM  
332 suggests that the change in cladoceran assemblage in 1958/1961 is a critical transition (Fig. 6\_DLM  
333 c).

334

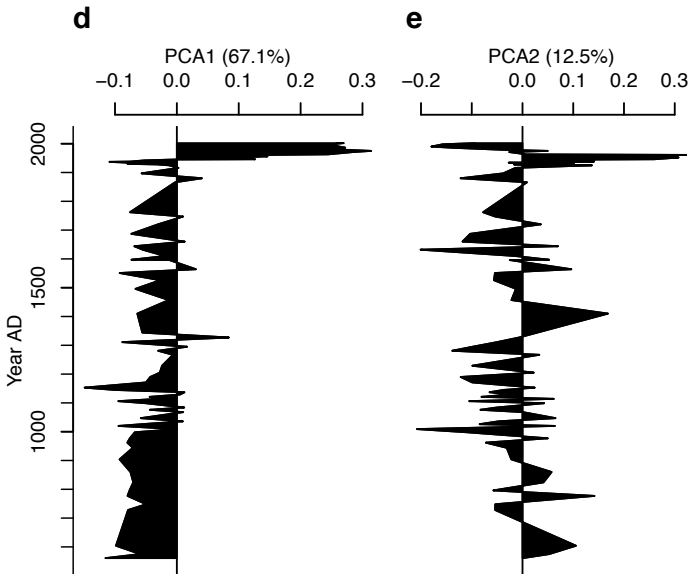
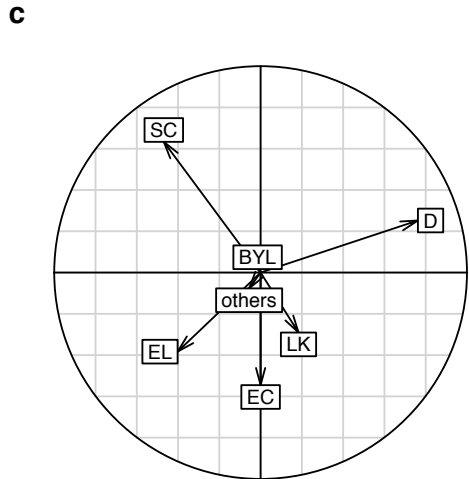
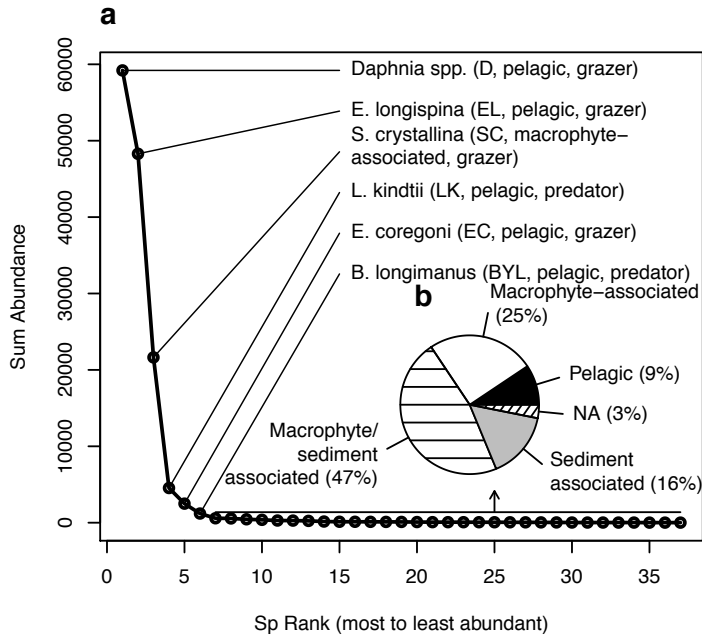
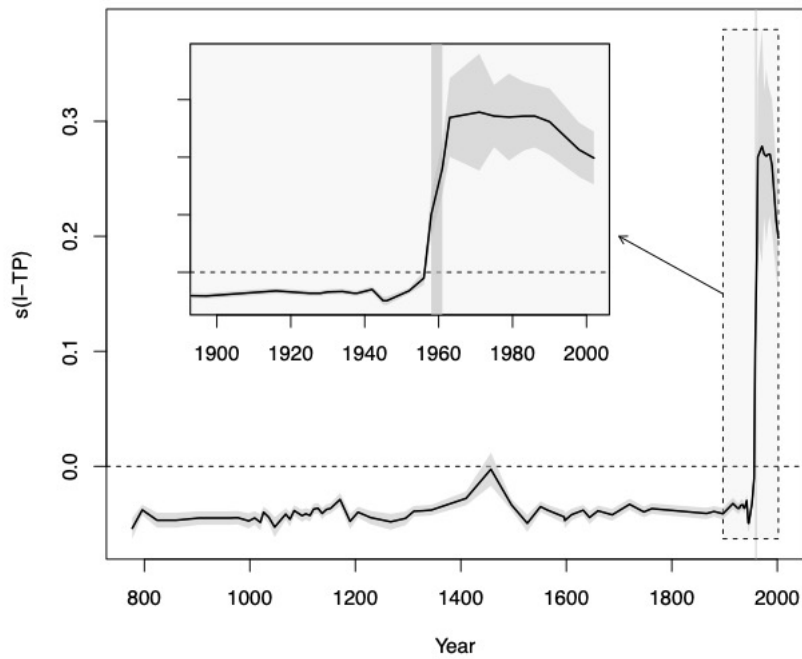
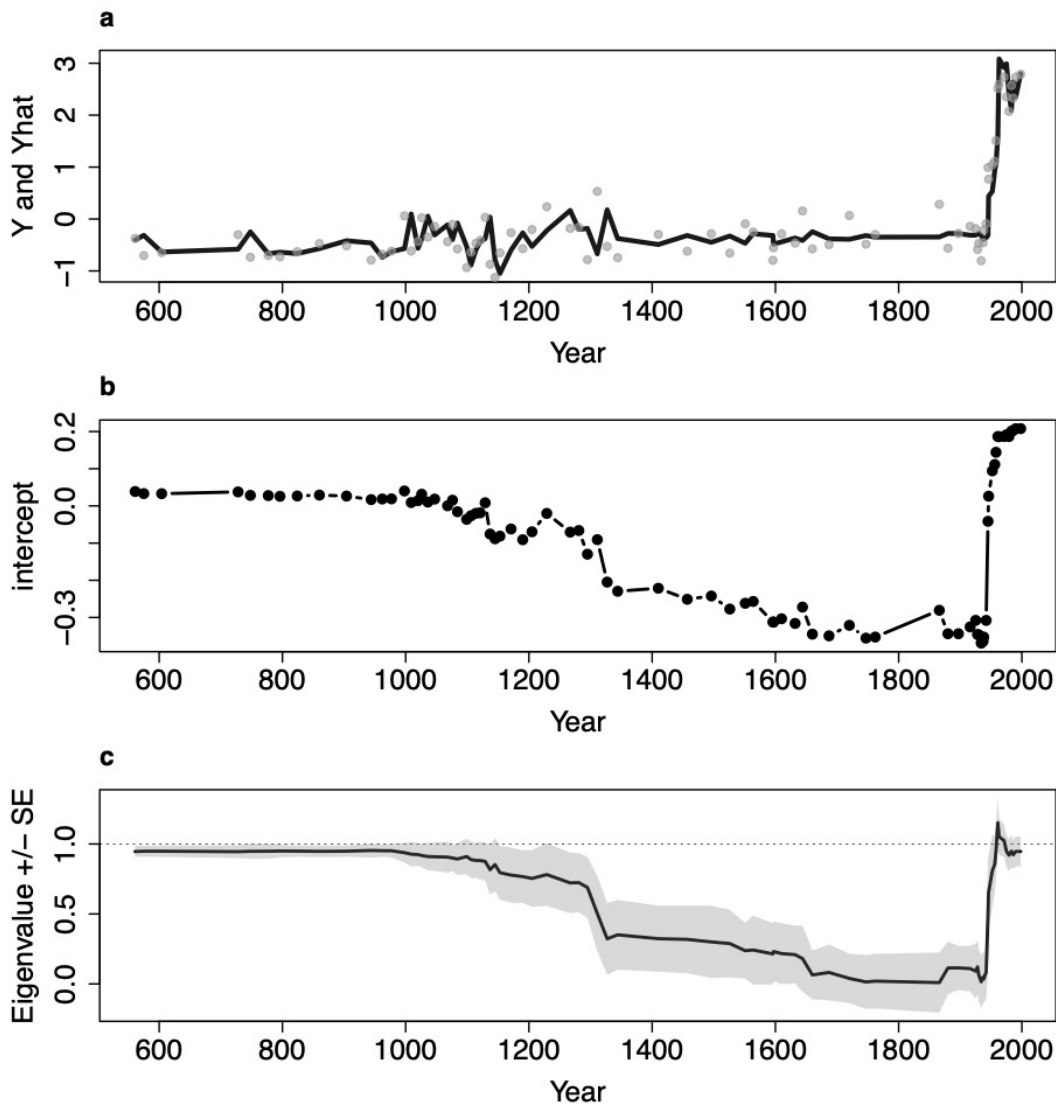


**Figure 4\_PCA.** (a) Ranking of species by abundances; (b) frequency of habitat for species that rank 7 to 37 in abundance; these low abundant species are grouped as “others” in the PCA. (c-e) Results from the PCA. (c) cocircle showing contribution of species to the first factorial plan. (d) PC1 and (e) PC2 scores over the years. Species code: SC: *Sida crystallina* var. *limnetica*, CH: *Chydorus* sp., EL: *Eubosmina longispina*, EC: *Eubosmina coregoni*, BYL: *Bythotrephes longimanus*, LK: *Leptodora kindtii*, BL: *Bosmina longirostris*, D: *Daphnia* spp.



335

336 **Figure 5\_GAM.** Temporal contribution of I-TP ( $s(I-TP)$ ) to PC1 with approximately 95% pointwise  
 337 confidence intervals to the contribution. Where the band includes the dashed zero line, the  
 338 contribution of the covariate is not statistically significantly different from the intercept.



339

340 **Figure 6\_DLM.** Summary of online dynamic linear model (DLM) results for Lake Geneva (n =  
 341 81). (a) The time series (grey points), goodness of fit (black line), (b) intercept, and (c) eigenvalue  
 342 (black line) with standard error (shaded area) are shown.

343

### 344 **Discussion**

345 We show that from 563 AD until the beginning of the 20<sup>th</sup> century, the ecological state of Lake  
 346 Geneva as depicted by cladoceran assemblages remained stable despite the climate variability of  
 347 3°C evidenced by local reconstructions (Fig. 3\_DESCRIPTIFa) (Büntgen et al. 2006). TP levels  
 348 remained low indicating a good buffering capacity of the system in regards to the land occupation  
 349 in the Alpine area over this period (Kaplan et al. 2009). The sediment archive mirrored the well-  
 350 documented eutrophication phase in Lake Geneva, that started at low levels of TP (< 10 µg P.l<sup>-1</sup>)

351 and led to the dominance of pelagic taxa. As TP concentrations are decreasing since the 1980s, the  
352 macrophytic-associated specie *S. crystallina* is not recovering and instead, the predatorous *L. kindtii*  
353 represent now a larger proportion of the assemblage (Fig. 3\_DESCRIPTIF). DLM revealed a critical  
354 transition in 1958-1961, for I-TP levels around 12-16  $\mu\text{g.l}^{-1}$ . It happened ca. 9 years before the  
355 critical transition identified for the oxygen level by Taranu *et al.* (2018). Lake Geneva hypoxic  
356 volume regime is one of the case study in the paper presenting the method. The driver for the critical  
357 transition in oxygen level was also attributed to eutrophication (Jenny *et al.* 2014; Taranu *et al.*  
358 2018). The “recent” cladoceran assemblage is radically different from the one characteristic of the  
359 563–1940 period, underlying the relevance of paleolimnological tools even for lakes that have been  
360 continuously surveyed as early as the late 1950s such as Lake Geneva. We show that from 563 AD  
361 until the beginning of the 20<sup>th</sup> century, the ecological state of Lake Geneva as depicted by cladoceran  
362 assemblages remained stable despite the climate variability of 3°C evidenced by local  
363 reconstructions (Büntgen *et al.* 2006). TP levels remained low indicating a good buffering capacity  
364 of the system in regards to the land occupation in the Alpine area over this period (Kaplan *et al.*  
365 2009). The sediment archive mirrored the well-documented eutrophication phase in Lake Geneva,  
366 that started at low levels of TP ( $< 10 \mu\text{g P.l}^{-1}$ ) and led to the dominance of pelagic taxa. As TP  
367 concentrations are decreasing since the 1980s, the macrophytic-associated specie *S. crystallina* is  
368 not recovering and instead, the predatorous *L. kindtii* represent now a larger proportion of the  
369 assemblage (Fig. 3\_DESCRIPTIF). DLM revealed a critical transition in 1958-1961, for I-TP levels  
370 around 12-16  $\mu\text{g.l}^{-1}$ . It happened ca. 9 years before the critical transition identified for the oxygen  
371 level by Taranu *et al.* (2018). Lake Geneva hypoxic volume regime is one of the case studies in the  
372 paper presenting the method. The driver for the critical transition in oxygen level was also attributed  
373 to eutrophication (Jenny *et al.* 2014; Taranu *et al.* 2018). The “recent” cladoceran assemblage is  
374 radically different from the one characteristic of the 563–1940 period, underlying the relevance of  
375 paleolimnological tools even for lakes that have been continuously surveyed as early as the late  
376 1950s such as Lake Geneva.

377

### 378 *Potential processes lost with the critical transition*

379 Large lakes are not typically considered as vulnerable to critical transitions between stable states,  
380 because most feedbacks associated with stable states are linked to some extent to the littoral zone  
381 (e.g., connection with sediment that includes resuspension of particles and remobilization of  
382 phosphorus, Hilt 2015). Other research suggests the threshold may be lower (Hilt *et al.* 2010), and

383 that the focus on the pelagic zone in deep lakes may overlook the role of the benthic and littoral  
384 zone (Vander Zanden and Vadeboncoeur 2002). The timing of eutrophication matches the loss of  
385 the littoral zone and the strengthening of the top-down control. Littoral areas could be functionally  
386 crucial components of habitat heterogeneity, biodiversity, and resilience, even in a large and deep  
387 lake for which their representability is always minor. The almost complete disappearance of *S.*  
388 *crystallina* remains after 1961 AD is consistent across pelagic cores (see Alric et al. 2013 Fig.  
389 4\_PCA), but also across lakes sharing the same timing of eutrophication (Lake Maggiore, Manca et  
390 al. 2007; Lake Bourget, Alric et al. 2013; Lake Lugano, unpublished data). *S. crystallina*, *Daphnia*  
391 spp., and *Eubosmina* sp. all graze on phytoplankton. The community lost the former of these grazers  
392 (reduced horizontal diversity) and gained a predator, *L. kindtii*, increasing its vertical diversity. *L.*  
393 *kindtii* was a consistent component of the assemblage but its relative abundance was <1% until the  
394 1980s (>10% of the assemblage). High horizontal and vertical diversity respectively increase and  
395 decrease stability to large perturbations (Zhao et al. 2019). The new planktonic food web structure  
396 of Lake Geneva makes it in theory less resilient to future large perturbations. Species interactions  
397 (and specifically, predation), were also found to mediate community response to large perturbation  
398 (drought); these responses were amplified at lower elevations, representing warmer climate in the  
399 space-for-time approach used by the authors (Amundrud and Srivastava 2019).

400 If the littoral zone is key to the resistance of Lake Geneva to past climatic variability, then the effort  
401 to restore the littoral areas should be sustained. Lake Geneva charophytic vegetation shows sign of  
402 recovery (Perfetta 2011). Charophytic vegetation is recovering faster than macrophytic beds because  
403 they depend solely on water to absorb nutrients (Perfetta 2011). However, restoration of the littoral  
404 vegetation is not solely a function of the nutrient concentration, but also urban infrastructure  
405 (rockfill, seawalls, channelling of small tributary streams, ...) and harbours.

406

#### 407 *Multiple yet asynchronous drivers: interactive carryover*

408 Eutrophication drove the major habitat and species change in Lake Geneva, as in the overwhelming  
409 number of cases for lakes (Carpenter 2005). More generally, land use is responsible for most of the  
410 negative impacts across terrestrial and freshwater ecosystem (e.g., Bajard et al. 2018). However  
411 climate change is increasingly exacerbating the impact of other drives on nature and human well-  
412 being (IPBES 2019). Our study shows that Lake Geneva is no exception to the trend. After 1,200  
413 years of ecological stability despites changes in air temperature, relatively low levels of phosphorus

414 triggered a critical transition in the system. It seems that before the 1950s, the ecological status of  
415 Lake Geneva, as mirrored by cladoceran (and diatoms, see Supplementary Materials S2)  
416 communities, was not vulnerable to changes of 3°C in air temperature and its consequent effects on  
417 lake water temperature. Indeed, SAT anomalies fluctuated within a range of 3°C over the period  
418 800-1800 AD alone in Central Europe (Büntgen et al. 2006), which falls into the same amplitude as  
419 the variations observed over the 20<sup>th</sup> and 21<sup>st</sup> centuries (Fig. 4\_PCAa&b). However, at the scale of  
420 the past 150 years, the same method (sediment remain analysis, ordination, GAM) revealed that  
421 climate warming was a significant driver of cladoceran (Alric et al. 2013) and diatoms (Berthon et  
422 al. 2014) assemblages. Our conjecture is that vulnerability to climate variability has changed  
423 following the critical transitions. Alric *et al.* (2013) and Berthon *et al.* (2014), working at the scale  
424 of the past 150 years, were able to quantify vulnerability to climate, while our sample  
425 disproportionately represent the period of resistance (pre-20<sup>th</sup> century), and thus the decoupling  
426 between climatic signal and ecological response.

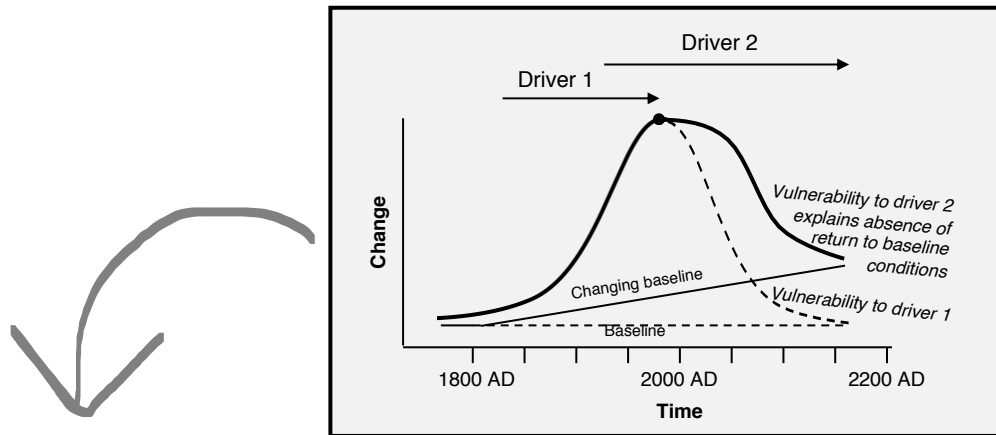
427 Ryo et al. (2019) conceptualize and review examples of such interactive carryover, i.e., when a prior  
428 driver changes an internal parameter or mechanism of a system, which lead the system to respond  
429 to a posterior driver differently (more, or less, depending whether drivers act synergistically or  
430 antagonistically) from how it would have responded without the experience of the first driver (Fig.  
431 7\_CONCEPT). The fact that air temperature increased to the same rate (+0.4°C per decade) and  
432 amplitude of anomalies (+2°C) in the 1930-1950s, without triggering the same responses, supports  
433 that hypothesis. Ecological vulnerability to climate change would not only be tied to the rate at  
434 which water is warming but also to inherited local human alterations of the lake food web. This  
435 conclusion is corroborated by a recent diachronic approach conducted at the neighboring,  
436 oligotrophic Lake Annecy under the same climatic context, where the lake surface water  
437 temperature has increased by 4°C between the 1970s and the 2000s (+2.5°C in Lake Geneva) but  
438 the cladoceran assemblage has barely responded to the change (Perga et al. 2015).

439 The idea that in the face of multiple stressors, addressing local or regional drivers could build  
440 resilience to continued global change, is often presented (Rockström et al. 2009; Scheffer et al.  
441 2015a; Rocha et al. 2015). If two drivers have similar impacts on the ecosystem, then the level of  
442 driver 1 that allows the systems to operate in its safe operate state under low levels of driver 2, may  
443 be too much if driver 2 increases (Scheffer et al. 2015a). Conversely, if local stressors already  
444 modified the ecosystem, its response to decreasing driver may not result in a return to the exact  
445 same baseline, because climate change (or another driver) may have changed these boundary  
446 conditions (Fig. 7\_CONCEPTa, Battarbee et al. 2005). Our findings expand this idea. In here, we

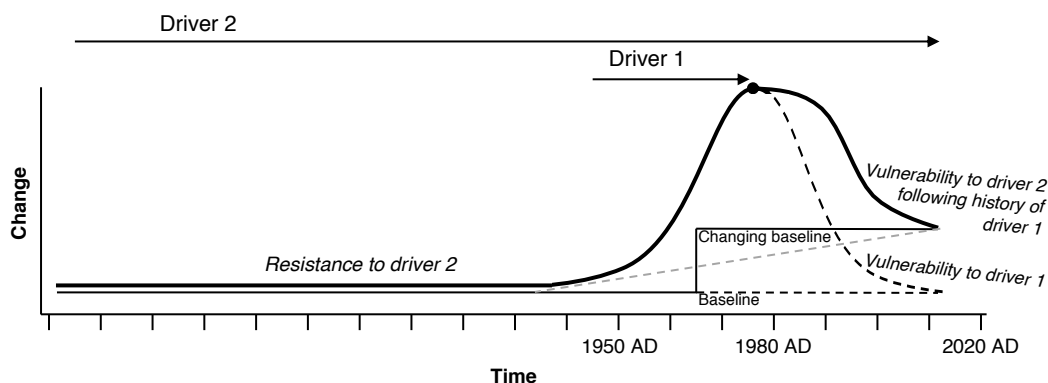
447 show that eutrophication actually acted as a switch from a regime of resistance to a new regime of  
448 frequent restructuration, and a different, more vertical, food web structure. If local drivers have to  
449 be reduced to build resilience, it needs to be done before the ecosystem has been pushed beyond its  
450 limits (Fig. 7\_CONCEPTb). The idea that in the face of multiple stressors, addressing local or  
451 regional drivers could build resilience to continued global change, is often presented (Rockström et  
452 al. 2009; Scheffer et al. 2015a; Rocha et al. 2015). If two drivers have similar impacts on the  
453 ecosystem, then the level of driver 1 that allows the systems to operate in its safe operate state under  
454 low levels of driver 2, may be too much if driver 2 increases (Scheffer et al. 2015a). Conversely, if  
455 local stressors already modified the ecosystem, its response to decreasing driver may not result in a  
456 return to the exact same baseline, because climate change (or another driver) may have changed  
457 these boundary conditions (Fig. 7\_CONCEPTa, Battarbee et al. 2005). Our findings expand this  
458 idea. In here, we show that eutrophication acted in fact as a switch from a regime of resistance to a  
459 new regime of frequent restructuration, and a different, more vertical, food web structure. As a  
460 consequence, if local drivers must be reduced to build resilience, it needs to be done before the  
461 ecosystem has been pushed beyond its limits (Fig. 7\_CONCEPTb).

462

a. Change in the boundary conditions (Battarbee *et al.* 2005)



b. Interactive carryover (Ryo *et al.* 2019)



Driver 2 = 0  
 Driver 2 + Driver 1 = 1

463

464 **Figure 7\_CONCEPT.** (a) Idealized diagram illustrating temporal ecological response of Lake  
 465 Geneva to increasing and decreasing drivers, freely adapted from Battarbee *et al.* (2005). They  
 466 concluded that new baseline conditions should be targeted in restoration programs because of the  
 467 juxtaposition of several forcings. (b) Our findings suggest the baseline may have changed as a  
 468 tipping point. As a perspective, we question whether vulnerability to driver 2 (e.g., climate) is true  
 469 only after driver 1 (e.g., eutrophication) decreased the resilience of the system.

470

471 *Time perspective and implication for managers*

472 Ecosystems evolve over timescales that are impossible to experience by a human eye, yet humans  
 473 are the ones responsible for their management (Vitousek *et al.* 1997). Ecologists acknowledge this  
 474 and there is no doubt long-term observatories provide invaluable knowledge on ecosystems  
 475 specificities and framework for ecological theories (Maberly *et al.* 2018). Our results show that Lake

476 Geneva long-term monitoring database, despite being one of the longest series in the world, may  
477 not be documenting the baseline condition. Further research should aim at deciphering whether the  
478 beginning of the monitoring captured a transient equilibrium (sensu Hastings et al. 2018), preceding  
479 the ecosystem crucial transition. Ecosystems evolve over timescales that are impossible to  
480 experience by a human eye, yet humans are the ones responsible for their management (Vitousek et  
481 al. 1997). Ecologists acknowledge this and there is no doubt long-term observatories provide  
482 invaluable knowledge on ecosystems specificities and framework for ecological theories (Maberly  
483 et al. 2018). Our results show that Lake Geneva long-term monitoring database, despite being one  
484 of the longest series in the world, may not be documenting the ecological baseline condition. Further  
485 research should aim at deciphering whether the beginning of the monitoring captured a transient  
486 equilibrium (sensu Hastings et al. 2018), preceding the ecosystem crucial transition.

487 The newest generation of managers may only know Lake Geneva as an ecosystem undergoing re-  
488 oligotrophication. Could this study lead to an example of “shifting baseline syndrome” (Pauly  
489 1995)? The syndrome, as first described in fisheries, arises when each generation of fisheries  
490 scientists accepts as a baseline the stock characteristics that occurred at the beginning of their career  
491 (Pauly 1995). In this case, the new generation of lake managers could accept as contemporary  
492 process the re-oligotrophication, and as history the eutrophication period. While Lake Geneva has  
493 now shifted long before the newest generation of lake managers was born, we should keep in mind  
494 the lake was once different. It is important to acknowledge this long history, to prevent increased  
495 tolerance for environmental degradation, and set appropriate baselines for conservation, restoration,  
496 and management (Soga and Gaston 2018). As a more general note, we realize that managers have  
497 the difficult job of making decisions that will trigger results they won’t see the total extent of within  
498 their lifetime. The short (at the scale of Lake Geneva history) eutrophication episode triggered long  
499 lasting effect in the ecological state of the system (interactive carryover, Ryo et al. 2019). The  
500 newest generation of managers only know Lake Geneva as a meso-oligotrophic system. Our results  
501 show the importance of accounting for longer ecosystem and lake trajectories (Wolkovich et al.  
502 2014).

503

#### 504 **Acknowledgment**

505 This work was supported by a PhD grant from the University Savoie-Mont Blanc to RB (VueLACC  
506 project). Dating was supported by Paleo5D and COOPERA (Region Auvergne-Rhône-Alpes)

507 grants. We thank the SOERE OLA-IS, INRA Thonon-les-Bains, CIPEL, 2017-03-21, developed by  
508 the INRA Eco-Informatics ORE, for the long-term monitoring data from Lake Geneva. We thank  
509 Anne-Lise Develle and Tiago A. Adrião Silva for their help in the geochemical analysis, Nicolas  
510 Thouveny and François Demory for providing access to facilities at the CEREGE paleomagnetic  
511 laboratory (Aix-Marseille University), and Stuart N. Lane for his constructive critical comments on  
512 a previous version of this manuscript.

513

#### 514 **Authors contribution**

515 RB, SG, MEP conceived the study and interpreted the results. RB, SG, KK, PS, CC, JLR conceived  
516 the age model. RB and AM analyzed the core sub-fossil samples. All authors contributed to the  
517 writing.

518 **Competing financial interests.** The authors declare no competing financial interests.

519

#### 520 **References**

- 521 Abram NJ, McGregor HV, Tierney JE, et al (2016) Early onset of industrial-era warming across the  
522 oceans and continents. *Nature* 536:411–418. <https://doi.org/10.1038/nature19082>
- 523 Alric B, Jenny J-P, Berthon V, et al (2013) Local forcings affect lake zooplankton vulnerability and  
524 response to climate warming. *Ecology* 94:2767–2780. <https://doi.org/10.1890/12-1903.1>
- 525 Alric B, Möst M, Domaizon I, et al (2016) Local human pressures influence gene flow in a  
526 hybridizing *Daphnia* species complex. *J Evol Biol* 29:720–735.  
527 <https://doi.org/10.1111/jeb.12820>
- 528 Amundrud SL, Srivastava DS (2019) Disentangling how climate change can affect an aquatic food  
529 web by combining multiple experimental approaches. *Glob Change Biol* 25:3528–3538.  
530 <https://doi.org/10.1111/gcb.14717>
- 531 Anneville O, Pelletier JP (2000) Recovery of Lake Geneva from eutrophication: quantitative  
532 response of phytoplankton. *Arch Hydrobiol* 607–624. [https://doi.org/10.1127/archiv-](https://doi.org/10.1127/archiv-hydrobiol/148/2000/607)  
533 [hydrobiol/148/2000/607](https://doi.org/10.1127/archiv-hydrobiol/148/2000/607)
- 534 Anneville O, Vogel C, Lobry J, Guillard J (2017) Fish communities in the Anthropocene: detecting  
535 drivers of changes in the deep peri-alpine Lake Geneva. *Inland Waters* 7:65–76.  
536 <https://doi.org/10.1080/20442041.2017.1294350>
- 537 Appleby PG, Richardson N, Nolan PJ (1991) 241Am dating of lake sediments. *Hydrobiologia*  
538 214:35–42. <https://doi.org/10.1007/BF00050929>

- 539 Arnaud F, Lignier V, Revel M, et al (2002) Flood and earthquake disturbance of  $^{210}\text{Pb}$   
540 geochronology (Lake Anterne, NW Alps). *Terra Nova* 14:225–232.  
541 <https://doi.org/10.1046/j.1365-3121.2002.00413.x>
- 542 Bajard M, Etienne D, Quinsac S, et al (2018) Legacy of early anthropogenic effects on recent lake  
543 eutrophication (Lake Bénit, northern French Alps). *Anthropocene* 24:72–87.  
544 <https://doi.org/10.1016/j.ancene.2018.11.005>
- 545 Battarbee RW, John Anderson N, Jeppesen E, Leavitt PR (2005) Combining palaeolimnological  
546 and limnological approaches in assessing lake ecosystem response to nutrient reduction.  
547 *Freshw Biol* 50:1772–1780. <https://doi.org/10.1111/j.1365-2427.2005.01427.x>
- 548 Berthon V, Alric B, Rimet F, Perga M-E (2014) Sensitivity and responses of diatoms to climate  
549 warming in lakes heavily influenced by humans. *Freshw Biol* 59:1755–1767.  
550 <https://doi.org/10.1111/fwb.12380>
- 551 Berthon V, Marchetto A, Rimet F, et al (2013) Trophic history of French sub-alpine lakes over the  
552 last ~150 years: phosphorus reconstruction and assessment of taphonomic biases. *J Limnol*  
553 72:34. <https://doi.org/10.4081/jlimnol.2013.e34>
- 554 Blaauw M (2010a) clam version 2.2
- 555 Blaauw M (2010b) Methods and code for ‘classical’ age-modelling of radiocarbon sequences. *Quat*  
556 *Geochronol* 5:512–518. <https://doi.org/10.1016/j.quageo.2010.01.002>
- 557 Blaauw M, Christen (2011) Flexible Paleoclimate Age-Depth Models Using an Autoregressive  
558 Gamma Process. *Bayesian Anal* 6:457–474
- 559 Bradley RS, Wanner H, Diaz HF (2016) The Medieval Quiet Period. *The Holocene*.  
560 <https://doi.org/10.1177/0959683615622552>
- 561 Bruel R, Marchetto A, Bernard A, et al (2018) Seeking alternative stable states in a deep lake.  
562 *Freshwater Biology*. <https://doi.org/10.1111/fwb.13093>
- 563 Büntgen U, Frank DC, Nievergelt D, Esper J (2006) Summer Temperature Variations in the  
564 European Alps, A.D. 755–2004. *J Clim* 19:5606–5623. <https://doi.org/10.1175/JCLI3917.1>
- 565 Büntgen U, Myglan VS, Ljungqvist FC, et al (2016) Cooling and societal change during the Late  
566 Antique Little Ice Age from 536 to around 660 AD. *Nat Geosci* 9:231–236.  
567 <https://doi.org/10.1038/ngeo2652>
- 568 Carpenter SR (2005) Eutrophication of aquatic ecosystems: Bistability and soil phosphorus. *Proc*  
569 *Natl Acad Sci* 102:10002–10005. <https://doi.org/10.1073/pnas.0503959102>
- 570 CIPEL (2007) Plan d’action 2001-2010 en faveur du Léman, du Rhône et de leurs affluents “Pour  
571 que vivent le Léman et ses rivières” - tableau de bord technique. CIPEL
- 572 CIPEL (2010) Plan d’action 2011-2020 en faveur du Léman, du Rhône et de leurs affluents  
573 “Préserver le Léman, ses rives et ses rivières aujourd’hui et demain” - tableau de bord  
574 technique. CIPEL

- 575 CIPEL (2018) Rapports sur les études et recherches entreprises dans le bassin lémanique. CIPEL,  
576 Nyon
- 577 Crouzet C, Wilhelm B, Sabatier P, et al (2019) Palaeomagnetism for chronologies of recent alpine  
578 lake sediments: successes and limits. *J Paleolimnol* 62:259–278.  
579 <https://doi.org/10.1007/s10933-019-00087-z>
- 580 Crowley TJ, Lowery TS (2000) How Warm Was the Medieval Warm Period? *Ambio* 29:51–54.  
581 <https://doi.org/10.1579/0044-7447-29.1.51>
- 582 Davidson TA, Bennion H, Jeppesen E, et al (2011) The role of cladocerans in tracking long-term  
583 change in shallow lake trophic status. *Hydrobiologia* 676:299–315.  
584 <https://doi.org/10.1007/s10750-011-0851-9>
- 585 DeMott WR, Gulati RD (1999) Phosphorus limitation in *Daphnia*: Evidence from a long term study  
586 of three hypereutrophic Dutch lakes. *Limnol Oceanogr* 44:1557–1564.  
587 <https://doi.org/10.4319/lo.1999.44.6.1557>
- 588 Elser JJ, Hayakawa K, Urabe J (2001) Nutrient Limitation Reduces Food Quality for Zooplankton:  
589 *Daphnia* Response to Seston Phosphorus Enrichment. *Ecology* 82:898–903.  
590 [https://doi.org/10.1890/0012-9658\(2001\)082\[0898:NLRFQF\]2.0.CO;2](https://doi.org/10.1890/0012-9658(2001)082[0898:NLRFQF]2.0.CO;2)
- 591 Forel FA (1892) *Le Léman : monographie limnologique*. F. Rouge, Lausanne
- 592 Frey DG (1986) Cladocera analysis. In: *Handbook of holocene palaeoecology and palaeohydrology*,  
593 B.E. Berglund. Wiley & sons, Great Britain, pp 667–701
- 594 Hall RI, Smol JP (2010) Diatoms as indicators of lake eutrophication. In: *The Diatoms: Applications*  
595 *for the Environmental and Earth Sciences* 2nd edition, Cambridge University Press. Smol,  
596 J.P. & Stoermer, E.F., Cambridge, pp 122–151
- 597 Harris GP (1987) *Phytoplankton Ecology*. Springer Netherlands, Dordrecht
- 598 Hastings A, Abbott KC, Cuddington K, et al (2018) Transient phenomena in ecology. *Science*  
599 361:eaat6412. <https://doi.org/10.1126/science.aat6412>
- 600 Hessen DO, Færøvig PJ, Andersen T (2002) Light, Nutrients, and P:C Ratios in Algae: Grazer  
601 Performance Related to Food Quality and Quantity. *Ecology* 83:1886–1898.  
602 <https://doi.org/10.2307/3071772>
- 603 Hilt S (2015) Regime shifts between macrophytes and phytoplankton – concepts beyond shallow  
604 lakes, unravelling stabilizing mechanisms and practical consequences. *Limnetica* 34:467–  
605 480
- 606 Hilt S, Henschke I, Rucker J, Nixdorf B (2010) Can submerged macrophytes influence turbidity and  
607 trophic state in deep lakes? Suggestions from a case study. *Journal of Environmental Quality*  
608 39:728–733
- 609 Hodgson D, McDonald JL, Hosken DJ (2015) What do you mean, ‘resilient’? *Trends Ecol Evol*  
610 30:503–506. <https://doi.org/10.1016/j.tree.2015.06.010>

- 611 IPBES (2019) Summary for policymakers of the global assessment report on biodiversity and  
612 ecosystem services of the Intergovernmental Science-Policy Platform on Biodiversity and  
613 Ecosystem Services. IPBES secretariat, Bonn, Germany
- 614 Jenny J-P, Arnaud F, Alric B, et al (2014) Inherited hypoxia: A new challenge for reoligotrophicated  
615 lakes under global warming: Holocene hypoxia dynamics in large lakes. *Glob Biogeochem*  
616 *Cycles* 1–11. <https://doi.org/10.1002/2014GB004932>
- 617 Jolliffe IT (1986) *Principal Component Analysis*. Springer-Verlag, New York, NY, USA
- 618 Kaplan JO, Krumhardt KM, Zimmermann N (2009) The prehistoric and preindustrial deforestation  
619 of Europe. *Quat Sci Rev* 28:3016–3034. <https://doi.org/10.1016/j.quascirev.2009.09.028>
- 620 Kremer K, Corella JP, Adatte T, et al (2015) Origin of turbidites in deep Lake Geneva (France–  
621 Switzerland) in the last 1500 years. *J Sediment Res* 85:1455–1465.  
622 <https://doi.org/10.2110/jsr.2015.92>
- 623 Kremer K, Simpson G, Girardclos S (2012) Giant Lake Geneva tsunami in AD 563. *Nat Geosci*  
624 5:756–757. <https://doi.org/10.1038/ngeo1618>
- 625 Larsen LB, Vinther BM, Briffa KR, et al (2008) New ice core evidence for a volcanic cause of the  
626 A.D. 536 dust veil. *Geophys Res Lett* 35:. <https://doi.org/10.1029/2007GL032450>
- 627 Levin SA (1992) The Problem of Pattern and Scale in Ecology: The Robert H. MacArthur Award  
628 Lecture. *Ecology* 73:1943–1967. <https://doi.org/10.2307/1941447>
- 629 Ljungqvist FC (2010) A new reconstruction of temperature variability in the extra-tropical Northern  
630 hemisphere during the last two millennia. *Geogr Ann* 92:339–351.  
631 <https://doi.org/10.1111/j.1468-0459.2010.00399.x>
- 632 Maberly SC, Ciar D, Elliott JA, et al (2018) From Ecological Informatics to the Generation of  
633 Ecological Knowledge: Long-Term Research in the English Lake District. In: Recknagel F,  
634 Michener WK (eds) *Ecological Informatics*. Springer International Publishing, Cham, pp  
635 455–482
- 636 Manca MM, Torretta B, Comoli P, et al (2007) Major changes in trophic dynamics in large, deep  
637 sub-alpine Lake Maggiore from 1940s to 2002: a high resolution comparative palaeo-  
638 neolimnological study. *Freshw Biol* 52:2256–2269. <https://doi.org/10.1111/j.1365-2427.2007.01827.x>
- 640 Mann ME, Jones PhilipD (2003) Global surface temperatures over the past two millennia. *Geophys*  
641 *Res Lett* 30:. <https://doi.org/10.1029/2003GL017814>
- 642 Nauwerck A (1991) The history of the genus *Eubosmina* in Lake Mondsee (Upper Austria).  
643 *Hydrobiologia* 225:87–103
- 644 Pauly D (1995) Anecdotes and the shifting baseline syndrome of fisheries. *Trends in Ecology &*  
645 *Evolution* 10:430. [https://doi.org/10.1016/S0169-5347\(00\)89171-5](https://doi.org/10.1016/S0169-5347(00)89171-5)
- 646 Perfetta J (2011) *Macrophytes of Lake Geneva*. CIPEL, Genève

- 647 Perga M-E, Frossard V, Jenny J-P, et al (2015) High-resolution paleolimnology opens new  
648 management perspectives for lakes adaptation to climate warming. *Front Ecol Environ* 3:.  
649 <https://doi.org/10.3389/fevo.2015.00072>
- 650 Pole A, West M, Harrison J (1994) *Applied Bayesian forecasting and time series analysis*. Chapman  
651 and Hall, New York
- 652 Rocha JC, Peterson G, Bodin Ö, Levin S (2018) Cascading regime shifts within and across scales.  
653 *Science* 362:1379–1383. <https://doi.org/10.1126/science.aat7850>
- 654 Rocha JC, Peterson GD, Biggs R (2015) Regime Shifts in the Anthropocene: Drivers, Risks, and  
655 Resilience. *PloS One* 10:e0134639. <https://doi.org/10.1371/journal.pone.0134639>
- 656 Rockström J, Steffen W, Noone K, et al (2009) A safe operating space for humanity. *Nature*  
657 461:472–475. <https://doi.org/10.1038/461472a>
- 658 Ryo M, Aguilar-Trigueros CA, Pinek L, et al (2019) Basic Principles of Temporal Dynamics.  
659 *Trends in Ecology & Evolution* 34:723–733. <https://doi.org/10.1016/j.tree.2019.03.007>
- 660 Scheffer M, Barrett S, Carpenter SR, et al (2015a) Creating a safe operating space for iconic  
661 ecosystems. *Science* 347:1317–1319. <https://doi.org/10.1126/science.aaa3769>
- 662 Scheffer M, Carpenter SR (2003) Catastrophic regime shifts in ecosystems: linking theory to  
663 observation. *Trends Ecol Evol* 18:648–656. <https://doi.org/10.1016/j.tree.2003.09.002>
- 664 Scheffer M, Carpenter SR, Dakos V, van Nes EH (2015b) Generic Indicators of Ecological  
665 Resilience: Inferring the Chance of a Critical Transition. *Annu Rev Ecol Evol Syst* 46:145–  
666 167. <https://doi.org/10.1146/annurev-ecolsys-112414-054242>
- 667 Soga M, Gaston KJ (2018) Shifting baseline syndrome: causes, consequences, and implications.  
668 *Frontiers in Ecology and the Environment* 16:222–230. <https://doi.org/10.1002/fee.1794>
- 669 Szeroczyńska K, Sarmaja-Korjonen K (2007) *Atlas of subfossil Cladocera from central and northern*  
670 *Europe*. Friends of the Lower Vistula Society, Świecie
- 671 Tadolnéké RD, Lazzarotto J, Anneville O, Druart J-C (2009) Phytoplankton productivity increased  
672 in Lake Geneva despite phosphorus loading reduction. *J Plankton Res* 31:1179–1194.  
673 <https://doi.org/10.1093/plankt/fbp063>
- 674 Taranu ZE, Carpenter SR, Frossard V, et al (2018) Can we detect ecosystem critical transitions and  
675 signals of changing resilience from paleo-ecological records? *Ecosphere* 9:e02438.  
676 <https://doi.org/10.1002/ecs2.2438>
- 677 Urabe J, Clasen J, Sterner RW (1997) Phosphorus limitation of *Daphnia* growth: Is it real? *Limnol*  
678 *Oceanogr* 42:1436–1443
- 679 Vander Zanden MJ, Vadeboncoeur Y (2002) Fishes as integrators of benthic and pelagic food webs  
680 in lakes. *Ecology* 83:2152–2161
- 681 Vincent WF, Bertola C (2014) Lake Physics to Ecosystem Services: Forel and the Origins of  
682 Limnology. *Limnology and Oceanography e-Lectures* 4:1–47.  
683 <https://doi.org/10.4319/lo.2014.wvincent.cbortola.8>

- 684 Vitousek PM, Mooney HA, Lubchenco J, Melillo JM (1997) Human Domination of Earth's  
685 Ecosystems. *Science* 277:494–499
- 686 Willen E (1991) Planktonic diatoms - an ecological review. *Algological Studies* 62:69–106
- 687 Wolkovich EM, Cook BI, McLauchlan KK, Davies TJ (2014) Temporal ecology in the  
688 Anthropocene. *Ecol Lett* 17:1365–1379. <https://doi.org/10.1111/ele.12353>
- 689 Wood S (2016) mgcv: Mixed GAM Computation Vehicle with GCV/AIC/REML Smoothness  
690 Estimation
- 691 Wunsam S, Schmidt R (1995) A diatom-phosphorus transfer function for Alpine and pre-alpine  
692 lakes. *Mem Ist Ital Idrobiol* 53:85–99
- 693 Zhao Q, Brink PJV den, Carpentier C, et al (2019) Horizontal and vertical diversity jointly shape  
694 food web stability against small and large perturbations. *Ecol Lett* 22:1152–1162.  
695 <https://doi.org/10.1111/ele.13282>
- 696
- 697

1 **Reframing Lake Geneva ecological trajectory in a context of multiple but asynchronous**  
2 **drivers**

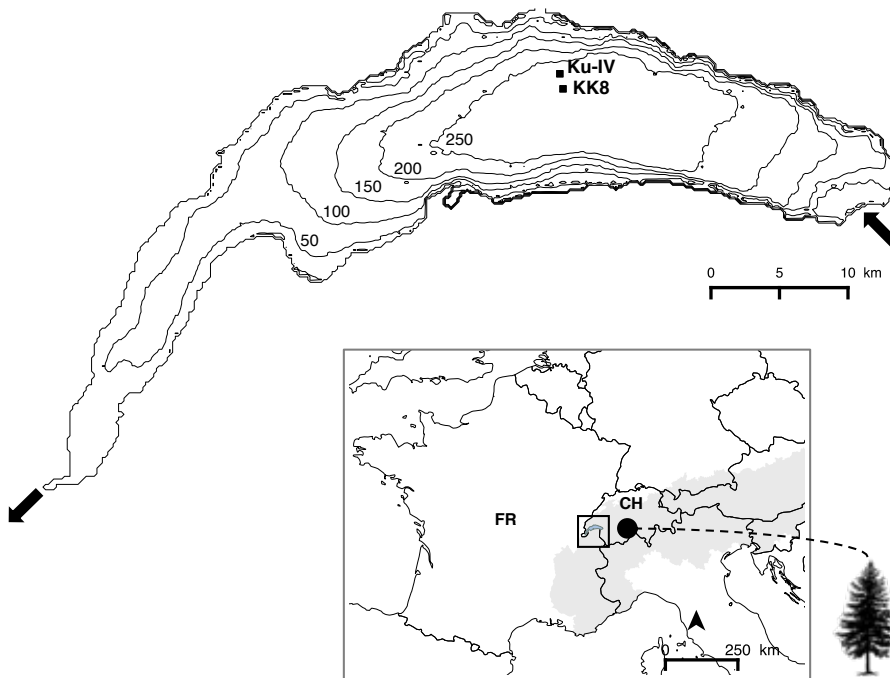
3

4 **Bruel et al.**

5 **Supplementary Material S1 – Lake Geneva sediment record**

6 **1. Sediment core sampling and approach**

7 We built a paleo-record dataset using two sediment cores collected in 2010 in the deepest basin  
8 of Lake Geneva. This Supplementary Material details the dating of the composite LEM10-CC  
9 from two cores (Ku-IV and KK8).



10 -

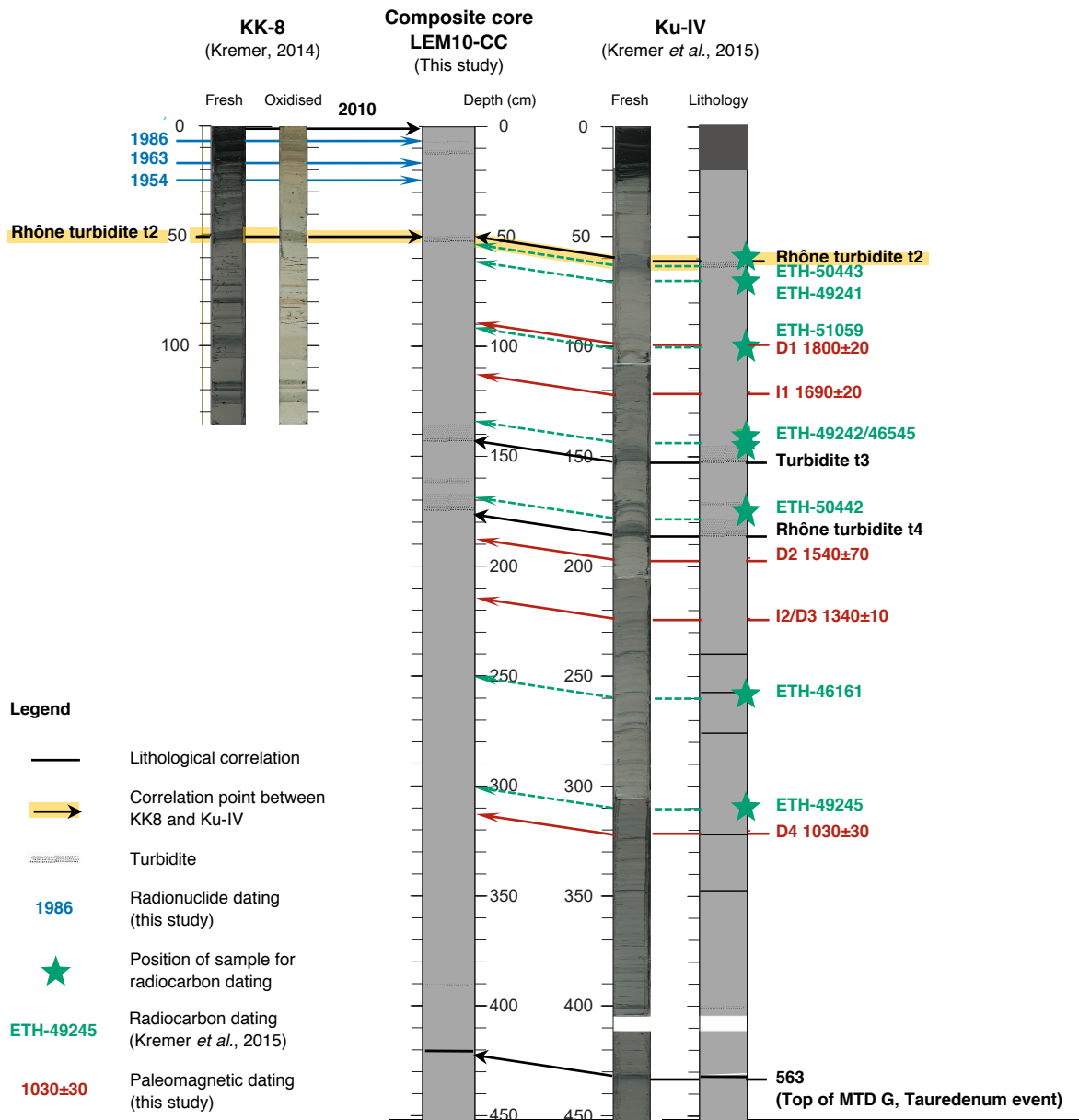
11 **Figure S1.1.** Lake Geneva lies at the border between France (FR) and Switzerland (CH) in the  
12 peri-alpine domain (Alps as grey surface on the bottom-right insert map). The bathymetry (in  
13 meters) and sediment core localization (black squares) are indicated. Arrows indicate the Rhône  
14 river inflow and outflow. The black circle on the bottom insert map shows the location of the  
15 four trees-ring sites used by Büntgen *et al.* (2006) to reconstruct SAT anomalies.

16

17 **2. Methods**

18 **2.1 Construction of the composite core LEM10-CC**

19 A paleo-record dataset was built using two sediment cores collected in 2010 in the deepest basin  
20 of Lake Geneva (Fig. 1). The main sediment archive is a long core covering the past 4,000 years  
21 (Ku-IV, 12 m, Long. E 6.60810/ Lat. N 46.47652, sampled on 02/09/2010) published by  
22 Kremer *et al.* (2012, 2015c). From this previously dated and studied core, only the 4.31 upper  
23 meters of the sediment sequence situated above the Tauredunum deposit of 563 AD  
24 documented by Kremer *et al.* (2012) were analyzed. As the top of Ku-IV was neither complete  
25 nor well preserved, the last ~100 years of the record could not be considered for this core. Thus,  
26 we used a short surface sediment cores as complementary archives to fill this gap. The short  
27 core, very similar to Ku-IV and located only 1.1 km southward, was used to solve the  
28 chronology issue of the past ca.100 years (KK8, 1.31 m, Long. E 6.61124/ Lat. N 46.46665,  
29 sampled on 19/04/2010). To build a coherent chronology, the two closely spaced sediment  
30 records were merged into one composite record LEM10-CC using the stratigraphic level of  
31 turbidite t2 (47.5-51.5 cm on KK8, 54.5-61.5 cm on Ku-IV) as identified by Kremer *et al.*  
32 (2015a) in both records.



33

34 **Figure S1.2.** Construction of the composite LEM10-CC sediment record with core photographs  
 35 and lithology description used in this study. From left to right, KK-8 (fresh sediment), KK8  
 36 (oxidized sediment), LEM10-CC composite record (lithology), Ku-IV (fresh sediment), Ku-IV  
 37 (lithology). The lithological correlations are represented with black lines and arrows. Dated  
 38 horizons are represented by blue ( $^{137}\text{Cs}$  activity peaks), red (paleomagnetism) and green  
 39 (radiocarbon) lines and arrows, and stars, respectively (see legend); the corresponding ages are  
 40 written next to the horizons.

41

## 42 2.2 Age model of LEM10-C

43 From the event free composite record LEM10-CC (see below), we calculated a continuous age-  
44 depth relationship with the R-code package ‘Clam’ version 2.2 (Blaauw 2010a) and compared  
45 the output with the Bayesian model ‘Bacon’ (Blaauw and Christen 2011).

46

### 47 2.2.1 Removal of event layers

48 The chronology of the composite core LEM10-CC is based on short-lived radionuclide  
49 activities, paleomagnetic secular variations, the coring year and a historical event. From the  
50 original 4.21-m-long composite core LEM10-CC, seven event layers with thickness above 1  
51 cm were interpreted as instantaneous events (Kremer et al. 2015a). They were thus removed  
52 from the raw sequence to construct a 3.93-m-long event-free composite core (Wilhelm et al.  
53 2012). The depth and thickness of these events, and details on the dating methods, are listed in  
54 Table S1.1.

55

56 **Table S1.1.** Core depth of event layers in original and composite sediment records along layer  
57 thickness. Last column include reference to identified instantaneous events in Kremer *et al.*  
58 (2015a) or radiocarbon dated material (Kremer et al. 2012).

Core where event layer was originally observed	Projected depth (cm) in composite LEM10-CC	Thickness of the event layer (cm)	Correlation with Kremer et al. <sup>5,7</sup>
KK8	6 – 7	1	
KK8	10.4 – 12.8	2.4	
KK8	47.5 – 51.5	4	t2, Rhône turbidite <sup>8</sup>
Ku-IV	135.5 – 142.5	7	
Ku-IV	162.5 – 166.5	4	
Ku-IV	170.5 – 179.5	7	<sup>14</sup> C age ETH-50442, t4 (Kremer et al. 2015a)
Ku-IV	391 – 393	2	<sup>14</sup> C age ETH-49245 (Kremer et al. 2015a)

59

### 60 2.3.2 Dating from radionuclide activity

61 The activity of short-lived radionuclides ( $^{210}\text{Pb}$ ,  $^{226}\text{Ra}$  and  $^{137}\text{Cs}$ ) was measured in the uppermost  
62 43 cm of core KK8, following a non-regular sampling step of 1 to 2 cm, in order to match facies  
63 boundaries, and using 0.3–2.4 g samples of dried sediment. Measurements were made by  
64 gamma spectrometry, using high-efficiency, very low background, well-type Ge detectors in  
65 the Modane underground laboratory (Reyss et al. 1995). The  $^{210}\text{Pb}$  *unsupported* excess activity  
66 ( $^{210}\text{Pbex}$ ) were calculated by subtracting the  $^{226}\text{Ra}$ -supported activity from the total  $^{210}\text{Pb}$   
67 activity. We then used the Constant Flux/Constant Sedimentation (CFCS) model applied to the  
68 decrease of  $^{210}\text{Pbex}$  to calculate a mean sedimentation rate (Goldberg 1963). The sedimentation  
69 rate uncertainties derived from the standard error of the linear regression of the CFCS model.

#### 70 2.2.2 Dating from paleomagnetic secular variations

71 The natural remanent magnetization (NRM) versus depth was measured in order to compare  
72 with known paleomagnetic secular variations such as Arch3k model (Donadini et al. 2009).  
73 Paleomagnetic investigations were performed on U-channel sub-samples of core Ku-IV, using  
74 a 3-axis, 2-G enterprise cryogenic magnetometer at the CEREGE laboratory (Aix-Marseille  
75 University, France). The NRM was progressively demagnetized using alternating field (AF) in  
76 10, 20, 30, 40 and 60 mT steps. The demagnetization diagrams (Zijderveld 1967) showed that  
77 behaviour was mainly unidirectional. Principal component analyses and calculation have been  
78 performed using puffin plot software (Lurcock and Wilson 2012) to calculate the Characteristic  
79 Remanent Magnetization (ChRM). Measurements affected by side effects (close to U-channel  
80 extremities) were removed. We also imparted and demagnetized the samples' anhysteretic and  
81 isothermal remanent magnetizations (ARM and IRM respectively) in order to ensure there is  
82 no change in magnetic mineralogy (see procedure in Wilhelm et al. 2016). Because the  
83 magnetic carrier properties were very stable along the entire studied section, we could be  
84 confident in the resulting ChRM direction.

#### 85 2.3.3 Historical event as stratigraphic marker

86 The base of the studied sediment sequence is the top of a large basin-wide mass movement  
87 deposit that has been related to the historical rockfall of 563 AD (“Tauredunum event”, Kremer  
88 et al. 2012).

#### 89 2.3.4 Radiocarbon dating

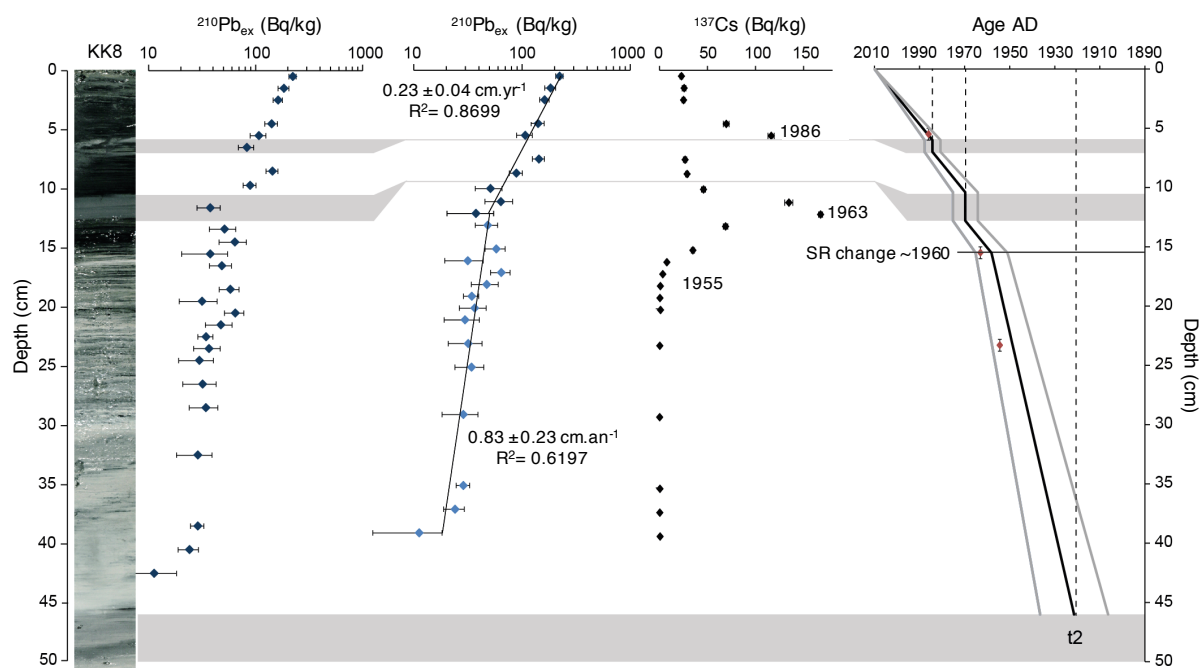
90 Samples of organic macro-remains were analyzed for radiocarbon dating (Kremer et al. 2012).

### 91 3. Results

#### 92 3.1 Chronology from radionuclides activity (1919-2010)

93 The excess  $^{210}\text{Pb}$  profile measured on core KK8 showed a regular decrease punctuated by two  
 94 drops in  $^{210}\text{Pb}_{\text{ex}}$  on the profile (Fig. S1.3). Following the lithology and Arnaud *et al.* (2002),  
 95 these low values of  $^{210}\text{Pb}_{\text{ex}}$  refer to instantaneous deposits (first two layers listed in Table S1.1)  
 96 and thus were excluded from the construction of the event-free sedimentary record.  $^{210}\text{Pb}_{\text{ex}}$   
 97 activities plotted on a logarithmic scale revealed two different mean sedimentation rates (SR),  
 98 respectively of  $0.23 \pm 0.04 \text{ cm.yr}^{-1}$  above 12.1 cm (event-free sequence) and  $0.83 \pm 0.23 \text{ mm.yr}^{-1}$   
 99 below this depth. Ages of the original sediment sequence provide a continuous age-depth  
 100 relationship with a main sedimentation change dated around 1960 AD. With this result, the age  
 101 of the event layer t2 (turbidite), initially determined from  $^{14}\text{C}$  dating as  $1785 \pm 115$  (Kremer *et al.*  
 102 *et al.* 2015a) is now much better constrained to  $1919.7 \pm 9.4$ .

103 The  $^{137}\text{Cs}$  activity profile of core KK8 reveals two peaks at  $5.5 \text{ cm} \pm 5 \text{ mm}$  and  $15.5 \text{ cm} \pm 5$   
 104 mm, corresponding respectively to 1986 (Chernobyl accident) and 1963 (atmospheric atomic  
 105 tests, Appleby *et al.* 1991). Below  $23.5 \text{ cm} \pm 5 \text{ mm}$ , the recorded  $^{137}\text{Cs}$  activities are close to  
 106 zero, pointing to a sequence deposited before 1955 (first  $^{137}\text{Cs}$  fallout). These three  $^{137}\text{Cs}$   
 107 markers are in good agreement with the CFCS age model over the last century, which confirms  
 108 its reliability (Fig. S1.3).



109  
 110 **Figure S1.3.** Chronology (with  $1\sigma$  uncertainties) of the uppermost part of core KK8 based on  
 111 activity of short-lived radionuclides ( $^{210}\text{Pb}_{\text{ex}}$  and  $^{137}\text{Cs}$ ) and the application of a CFCS model  
 112 to the event-free sedimentary profile of  $^{210}\text{Pb}_{\text{ex}}$  (right panel). Uncertainties of  $^{137}\text{Cs}$  activities  
 113 are included as dots size. A main sedimentation rate (SR) change appears around 1960 AD.

114 Grey bands correspond to event layers / turbidite intervals, interpreted as instantaneous deposits  
 115 (relatively to the rest of the chronology).

116

117 3.2 Record of paleomagnetic secular variations

118 The declination and inclination of the ChRM measured on Ku-IV were compared with those  
 119 issue for Arch 3k model (Donadini et al. 2009) in order to provide additional and independent  
 120 age depth coordinates. Assuming NRM is acquired during or immediately after deposition, this  
 121 comparison with reference curves allowed the identification of two inclination points and four  
 122 declination points (Table S1.2). Inclination points I1 ( $1690 \pm 20$ ) and I2 ( $1300 \pm 50$ ) were  
 123 respectively observed at  $121 \pm 10$  cm and  $221 \pm 15$  cm (Fig. S1.4) and declination points D1  
 124 ( $1800 \pm 20$ ), D2 ( $1540 \pm 70$ ), D3 ( $1370 \pm 40$ ) and D4 ( $1030 \pm 30$ ) were respectively observed  
 125 at  $100 \pm 15$  cm,  $196 \pm 15$  cm,  $224 \pm 10$  cm and  $322 \pm 10$  cm (Fig. S1.5). I2 and D3 were  
 126 observed for the same depth, thus allowing narrowing the confidence interval of the  $224 \text{ cm} \pm$   
 127  $10$  cm depth to an age of  $1340 \pm 10$  cm.

128

129 **Table S1.2.** The name of the stratigraphic horizons (ID), the dating method, the age and error  
 130 (cal. BP) are given along of the original core name, the respective projected depth in raw and  
 131 corrected composite record LEM10-CC. (ChRM = Characteristic Remanent Magnetization)

132 \* $^{14}\text{C}$  ages rejected by Kremer et al.(2012).

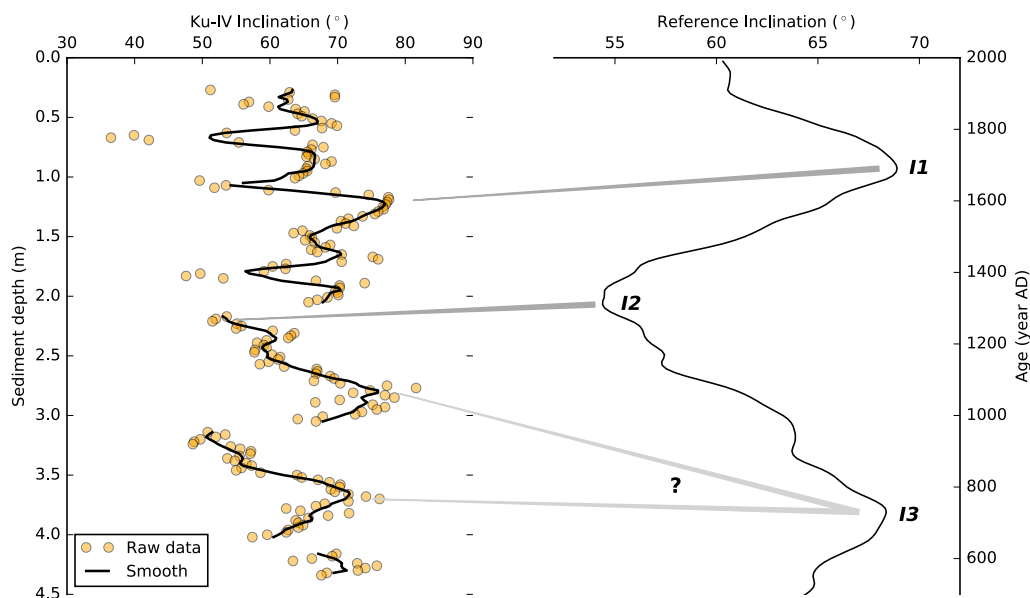
133 \*\* $^{14}\text{C}$  ages used to build the age-depth model by Kremer et al.(2012) but rejected in this study  
 134 in the light of new dated horizons.

135

ID	Dating Method	Age cal. BP (yr)	Original sediment core	Projected depth (cm) in LEM10-CC	Event corrected depth (cm) in LEM10-CC
Surface sediment	Coring year	$-60 \pm 1$	KK8	0	0
Chernobyl	$^{137}\text{Cs}$	$-36 \pm 1$	KK8	$5.5 \pm 0.5$	$5.5 \pm 0.5$
Atomic test	$^{137}\text{Cs}$	$-13 \pm 1$	KK8	$15.5 \pm 0.5$	$12.1 \pm 0.5$
Before test	$^{137}\text{Cs}$	$-5 \pm 1$	KK8	$23.5 \pm 0.5$	$20.1 \pm 0.5$
Rhône turbidite t2 (Kremer et al. 2015a)	$^{210}\text{Pb}$ decay	$30.3 \pm 9.4$	KK8	$47.5 \pm 0.5$	$44.1 \pm 0.5$

ETH-50443*	<sup>14</sup> C yr BP	143 ± 30	Ku-IV	52 ± 1	44.6 ± 1
ETH-49241*	<sup>14</sup> C yr BP	614 ± 51	Ku-IV	60 ± 1	51.6 ± 1
D1	ChRM	150 ± 10	Ku-IV	90 ± 7.5	82.6 ± 7.5
ETH-51059*	<sup>14</sup> C yr BP	382 ± 35	Ku-IV	90 ± 10	82.6 ± 10
I1	ChRM	260 ± 10	Ku-IV	111 ± 5	103.6 ± 5
ETH-49242*	<sup>14</sup> C yr BP	877 ± 59	Ku-IV	130 ± 1	122.6 ± 1
ETH-46545*	<sup>14</sup> C yr BP	870 ± 25	Ku-IV	135 ± 1	127.6 ± 1
ETH-50442**	<sup>14</sup> C yr BP	198 ± 30	Ku-IV	167 ± 1	144.6 ± 1
D2	ChRM	410 ± 35	Ku-IV	186 ± 7.5	160.6 ± 7.5
I2/D3	ChRM	610 ± 5	Ku-IV	214 ± 5	188.6 ± 5
ETH-46161**	<sup>14</sup> C yr BP	870 ± 25	Ku-IV	250 ± 10	224.6 ± 10
ETH-49245**	<sup>14</sup> C yr BP	1102 ± 72	Ku-IV	300.9 ± 3	273.6 ± 3
D4	ChRM	920 ± 15	Ku-IV	312 ± 5	286.6 ± 5
Tauredenum	Historical time marker (Kremer et al. 2012)	1387 ± 1	Ku-IV	421 ± 1	393.6 ± 1

136

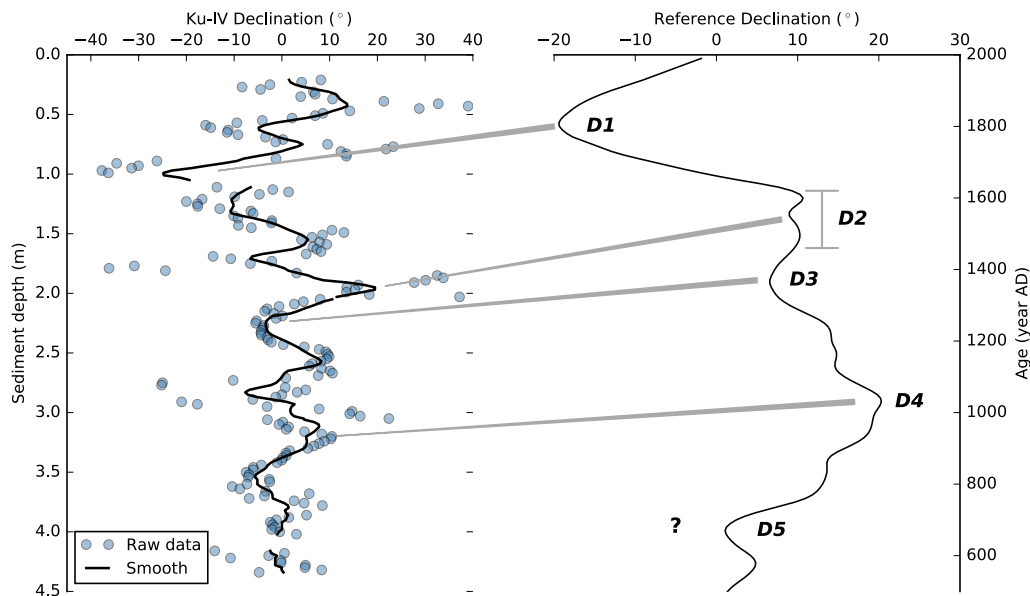


137

138 **Figure S1.4.** Inclination curve of Ku-IV averaged over a 12-cm-window (left panel) and  
 139 comparison with the reference inclination calculated from Arch3k model (Donadini et al. 2009)

140 for Lake Geneva (right panel). The I1 and I2 inclination points are used in the age-depth model  
141 (Figure S1.9).

142



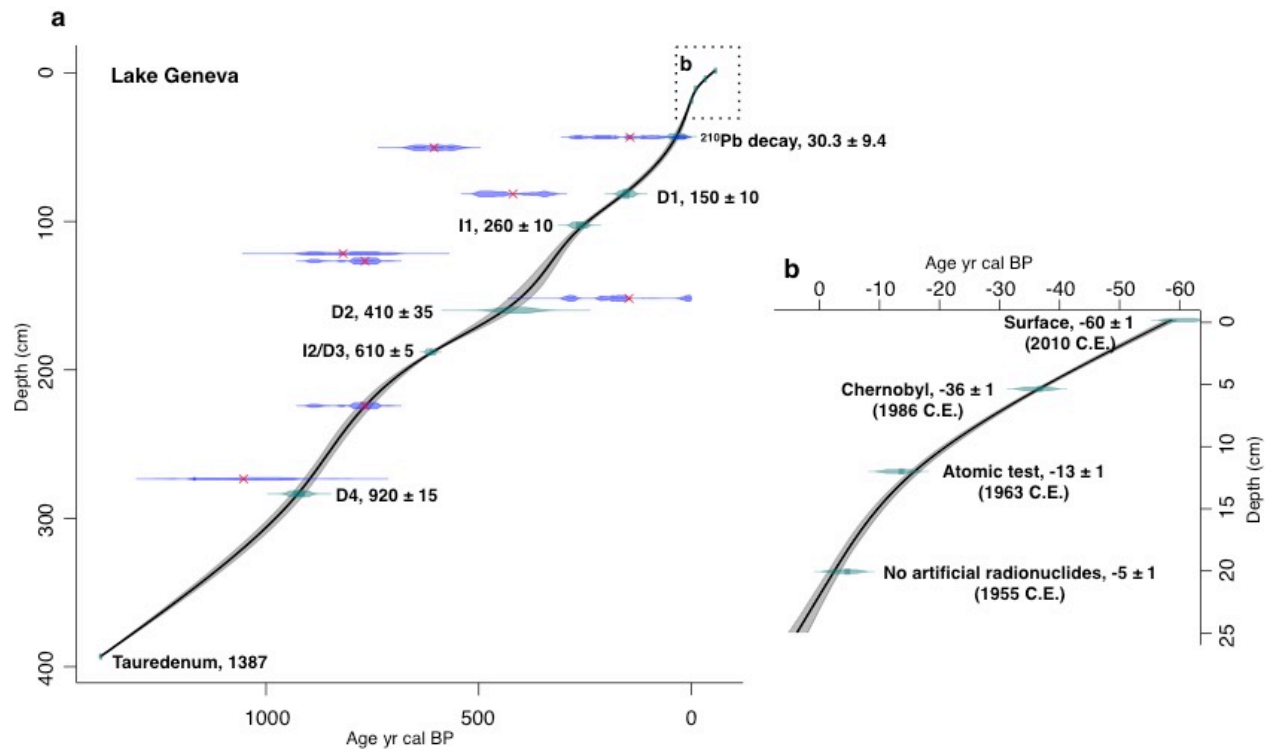
143

144 **Figure S1.5.** Declination curve of Ku-IV averaged over a 12-cm-window (left panel) and  
145 comparison with the reference declination calculated from Arch3k model(Donadini et al. 2009)  
146 for Lake Geneva (right panel). The D1 to D4 declination points are used in the age-depth model  
147 (Figure S1.9).

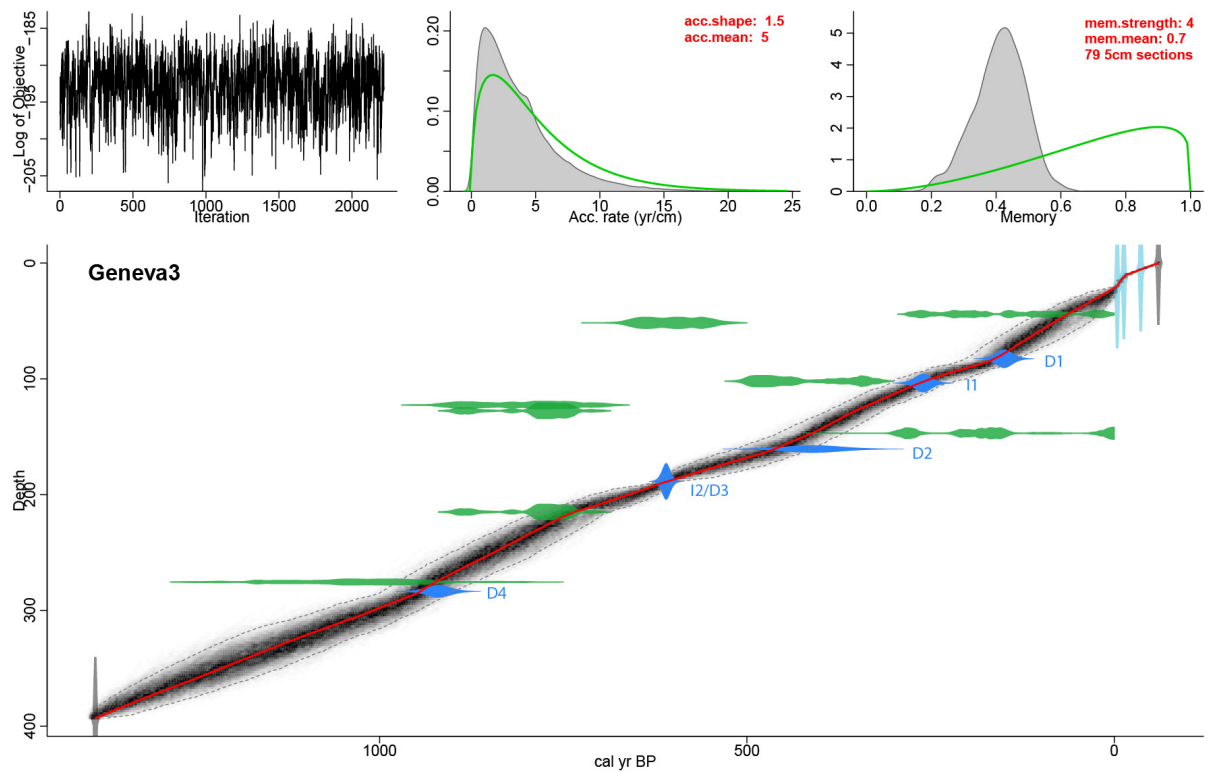
### 148 3.3 Age-depth model

149 From the event free composite core LEM10-CC, we calculated a continuous age-depth  
150 relationship with the R-code package ‘Clam’ version 2.2 (Blaauw 2010a). This age model  
151 integrates 11 stratigraphic horizons (Table S1.2): i) the coring year, ii) three time-markers from  
152  $^{137}\text{Cs}$  activity, iii) the age of turbidite t2 from  $^{210}\text{Pb}$  activity, iv) five dated points from the new  
153 paleomagnetic study, together with v) the 563 AD historical time marker. The chronology of  
154 the composite record LEM10-CC was already constrained on the 563-2010 time-period by the  
155 Tauredunum deposit event and the coring year. The new chronology add data from short-lived  
156 radionuclide activities and paleomagnetic secular variations allowing a rare dating precision in  
157 regards to the length of the core. The best Clam model was obtained using a smooth spline  
158 interpolation with a smoothing term of 0.32 which avoids sudden change in sedimentation rates  
159 (Fig S1.6). We also tested the age-depth model using the Bayesian model Bacon (Blaauw and

160 Christen 2011) with the same input data (Fig. S1.7). This independent Bacon model allows a  
 161 comparison with Clam model and shows that both curves have the same trend. The Clam model  
 162 was favored because it better fits the original time markers of radionuclides activity that are  
 163 important for a precise 20<sup>th</sup> century chronology.



164  
 165 **Figure S1.6.** Age-depth model of composite record LEM10-CC built with Clam R-code  
 166 package (Blaauw 2010b) from 11 stratigraphic horizons. **(a)** Total record and **(b)** zoom on the  
 167 three <sup>137</sup>Cs dates. Event layers with thickness above 1 cm were interpreted as instantaneous  
 168 events (Kremer et al. 2015a) and removed before the age model computation. The envelope  
 169 (grey area) represents the 2-sigma probability interval. Data not used to fit the age model are  
 170 marked with a red cross. See Supplementary Materials S1 for details.



171

172 **Figure S1.7.** Age-depth model of composite core LEM10-CC built with Bacon (Blaauw and  
 173 Christen 2011) (Tab. S.1). The upper left panel shows the iteration history, the upper middle  
 174 panel shows the prior (green line) and posterior (grey area) of the sediment accumulation rate  
 175 (yr/cm), and the upper right panel shows the prior (green line) and posterior (grey area) of the  
 176 memory (1 cm autocorrelation strength). The bottom panel indicates the age-depth model. The  
 177 solid red line represents the single ‘best’ model based on the weighted mean age for each depth.  
 178 Associated uncertainties are represented by the grayscale (the darker grey dots are indicative  
 179 for more likely ages and the dashed black lines indicate the model’s 95% probability intervals.  
 180 The age-depth model is built on the age of the surface sediments (grey) and individual ages  
 181 obtained from radionuclides (light blue), radiocarbon dating (green) and paleomagnetism  
 182 (blue).

183

#### 184 4. Discussion

##### 185 4.1 Validity of the age model

186 The LEM10-CC age model reveals younger ages than previously estimated (Kremer et al.  
 187 2015a). <sup>14</sup>C dates are typically older due to the classical effect of terrestrial organic  
 188 macroremain reworking in the catchment. On the other hand, paleomagnetic chronology may  
 189 be affected by the lock-in depth (i.e. the delay in acquisition of the primary magnetization), that

190 implies that sediments are systematically older than the geomagnetic feature they preserve  
191 (Sagnotti et al. 2005; Mellström et al. 2015). We chose the paleomagnetism dating over the  $^{14}\text{C}$   
192 dates because their uncertainties ranges at the centimeter scale (Katari et al. 2000), i.e. decadal  
193 scale in Lake Geneva, instead of century scale errors in the case of  $^{14}\text{C}$ . Besides, this paleo-  
194 magnetism based model intercepts the age error of the four  $^{14}\text{C}$  retained by Kremer *et al.* (2012),  
195 confirming their realism (Fig. S1.6). The final age model does not show any large change in  
196 the sedimentation rates along the 1450 year-record, and does not call for any more hypotheses.  
197 The comparison between the Clam- and Bacon-modelled age-depth curves points to the same  
198 chronological trend but the Clam model provide a better fit of the radionuclides activity  
199 markers. The 20<sup>th</sup> century chronology is essential in this study, hence Clam-model was chosen.

200

#### 201 4.2 Sedimentation rates

202 The resulting sedimentation rates obtained with the Clam age-depth model are of  $0.2 \text{ cm.yr}^{-1}$  to  
203  $0.3 \text{ cm.yr}^{-1}$  from 563 to 1913. From 1913 to 1968, sedimentation rate increases as and varies  
204 between  $0.5$  and  $1 \text{ cm.yr}^{-1}$ , corresponding to the change of core, which is interpreted as a  
205 difference in compaction due to both different coring methods and porosity. However a drastic  
206 -and unexpected for a top core interval- decrease towards smaller values around  $0.3 \text{ cm.yr}^{-1}$  is  
207 observed since the 1960's. Although coring locations of KK-8 and Ku-IV are located distally  
208 from the Dranse and Rhone River deltas (Kremer et al. 2015a, b), sedimentation rates follows  
209 a general trend also observed in seven cores located more proximally to the Rhone River delta  
210 (Silva et al. 2016). Indeed, deep Lake Geneva sediment is mainly driven by changes in the  
211 sedimentary load of the rivers (Loizeau and Dominik 2000). The recent decrease in  
212 sedimentation rate observed in this study but also in Silva *et al.* (2016), is certainly related to  
213 the decrease in the sediment load of the Rhone River system since the 1960s (Loizeau and  
214 Dominik 2000). This change in sediment load is explained by the strong modifications in the  
215 hydrology and sediment routing of the Rhône catchment (Bakker et al. 2017) that happened  
216 after the building of several major hydropower systems in Wallis (Loizeau and Dominik 2000).

217 The combination of different dating methods crossed with a good knowledge of Lake Geneva  
218 sedimentation dynamics (Loizeau and Dominik 2000) and hydrological historic events (Kremer  
219 et al. 2015a, b) allowed to build an age model for the sediment record with relatively low age  
220 error. This was crucial as we later compared the plankton dynamics reconstructed from the  
221 sediment to an independent climatic record (see main text).

222

223 **References**

- 224 Appleby PG, Richardson N, Nolan PJ (1991)  $^{241}\text{Am}$  dating of lake sediments. *Hydrobiologia*  
225 214:35–42. <https://doi.org/10.1007/BF00050929>
- 226 Arnaud F, Lignier V, Revel M, et al (2002) Flood and earthquake disturbance of  $^{210}\text{Pb}$   
227 geochronology (Lake Anterne, NW Alps). *Terra Nova* 14:225–232.  
228 <https://doi.org/10.1046/j.1365-3121.2002.00413.x>
- 229 Bakker M, Costa A, Silva TAA, et al (2017) Unraveling the effects of climate change and flow  
230 abstraction on an aggrading Alpine river. *Geophysical Research Abstracts* 19:
- 231 Blaauw M (2010a) Methods and code for ‘classical’ age-modelling of radiocarbon sequences.  
232 *Quat Geochronol* 5:512–518. <https://doi.org/10.1016/j.quageo.2010.01.002>
- 233 Blaauw M (2010b) clam version 2.2
- 234 Blaauw M, Christen (2011) Flexible Paleoclimate Age-Depth Models Using an Autoregressive  
235 Gamma Process. *Bayesian Anal* 6:457–474
- 236 Büntgen U, Frank DC, Nievergelt D, Esper J (2006) Summer Temperature Variations in the  
237 European Alps, A.D. 755–2004. *J Clim* 19:5606–5623.  
238 <https://doi.org/10.1175/JCLI3917.1>
- 239 Crouzet C, Wilhelm B, Sabatier P, et al (2019) Palaeomagnetism for chronologies of recent  
240 alpine lake sediments: successes and limits. *J Paleolimnol* 62:259–278.  
241 <https://doi.org/10.1007/s10933-019-00087-z>
- 242 Donadini F, Korte M, Constable CG (2009) Geomagnetic field for 0-3 ka: 1. New data sets for  
243 global modeling: GEOMAGNETIC FIELD FOR 0-3 KA, 1. *Geochem Geophys*  
244 *Geosyst* 10:1–28. <https://doi.org/10.1029/2008GC002295>
- 245 Goldberg ED (1963) Geochronology with  $^{210}\text{Pb}$  in radioactive dating. *International Atomic*  
246 *Energy Contribution* 1510:121–131
- 247 Katari K, Tauxe L, King J (2000) A reassessment of post-depositional remanent magnetism:  
248 preliminary experiments with natural sediments. *Earth Planet Sci Lett* 183:147–160
- 249 Kremer K, Corella JP, Adatte T, et al (2015a) Origin of turbidites in deep Lake Geneva (France–  
250 Switzerland) in the last 1500 years. *J Sediment Res* 85:1455–1465.  
251 <https://doi.org/10.2110/jsr.2015.92>
- 252 Kremer K, Corella JP, Hilbe M, et al (2015b) Changes in distal sedimentation regime of the  
253 Rhone delta system controlled by subaquatic channels (Lake Geneva,  
254 Switzerland/France). *Marine Geology* 370:125–135.  
255 <https://doi.org/10.1016/j.margeo.2015.10.013>
- 256 Kremer K, Hilbe M, Simpson G, et al (2015c) Reconstructing 4000 years of mass movement  
257 and tsunami history in a deep peri-Alpine lake (Lake Geneva, France-Switzerland).  
258 *Sedimentology* 62:1305–1327. <https://doi.org/10.1111/sed.12190>

- 259 Kremer K, Simpson G, Girardclos S (2012) Giant Lake Geneva tsunami in AD 563. *Nat Geosci*  
 260 5:756–757. <https://doi.org/10.1038/ngeo1618>
- 261 Loizeau J-L, Dominik J (2000) Evolution of the Upper Rhone River discharge and suspended  
 262 sediment load during the last 80 years and some implications for Lake Geneva. *Aquat*  
 263 *Sci* 54–67
- 264 Lurcock PC, Wilson GS (2012) PuffinPlot: A versatile, user-friendly program for  
 265 paleomagnetic analysis: TECHNICAL BRIEF. *Geochem Geophys Geosyst* 13:1–6.  
 266 <https://doi.org/10.1029/2012GC004098>
- 267 Mellström A, Nilsson A, Stanton T, et al (2015) Post-depositional remanent magnetization  
 268 lock-in depth in precisely dated varved sediments assessed by archaeomagnetic field  
 269 models. *Earth Planet Sci Lett* 410:186–196. <https://doi.org/10.1016/j.epsl.2014.11.016>
- 270 Reyss J-L, Schmidt S, Legeleux F, Bonté P (1995) Large, low background well-type detectors  
 271 for measurements of environmental radioactivity. *Nucl Instrum Methods Phys Res A*  
 272 357:391–397. [https://doi.org/10.1016/0168-9002\(95\)00021-6](https://doi.org/10.1016/0168-9002(95)00021-6)
- 273 Sagnotti L, Budillon F, Dinarès-Turell J, et al (2005) Evidence for a variable paleomagnetic  
 274 lock-in depth in the Holocene sequence from the Salerno Gulf (Italy): Implications for  
 275 “high-resolution” paleomagnetic dating: PALEOMAGNETIC LOCK-IN DEPTH.  
 276 *Geochem Geophys Geosyst* 6:1–11. <https://doi.org/10.1029/2005GC001043>
- 277 Silva TA, Girardclos S, Loizeau J-L (2016) Geochemical dataset of the Rhone River delta  
 278 sediments (Lake Geneva). Disentangling human impacts from climate change. AGU  
 279 Fall Meeting.
- 280 Wilhelm B, Arnaud F, Sabatier P, et al (2012) 1400 years of extreme precipitation patterns over  
 281 the Mediterranean French Alps and possible forcing mechanisms. *Quat Res* 78:1–12
- 282 Wilhelm B, Vogel H, Crouzet C, et al (2016) Frequency and intensity of palaeofloods at the  
 283 interface of Atlantic and Mediterranean climate domains. *Clim Past* 12:299–316.  
 284 <https://doi.org/10.5194/cp-12-299-2016>
- 285 Zijderveld JDA (1967) AC demagnetization of rock: analysis of results. In: *Methods in*  
 286 *Paleomagnetism*, Elsevier. Collinson, D.W., Creer, K.M., Runcorn, S.K., Amsterdam, pp  
 287 254–286
- 288

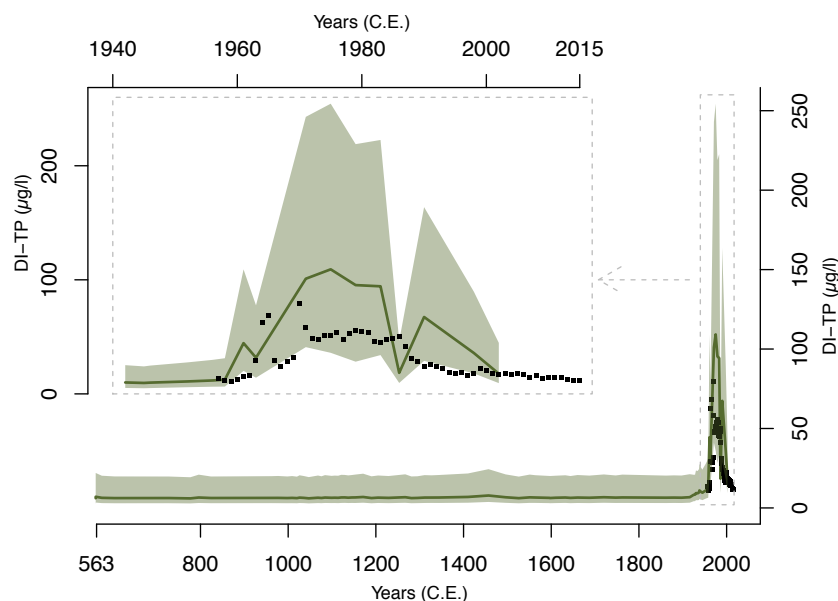
1 **Reframing Lake Geneva ecological trajectory in a context of multiple but asynchronous**  
2 **drivers**

3

4 **Bruel et al.**

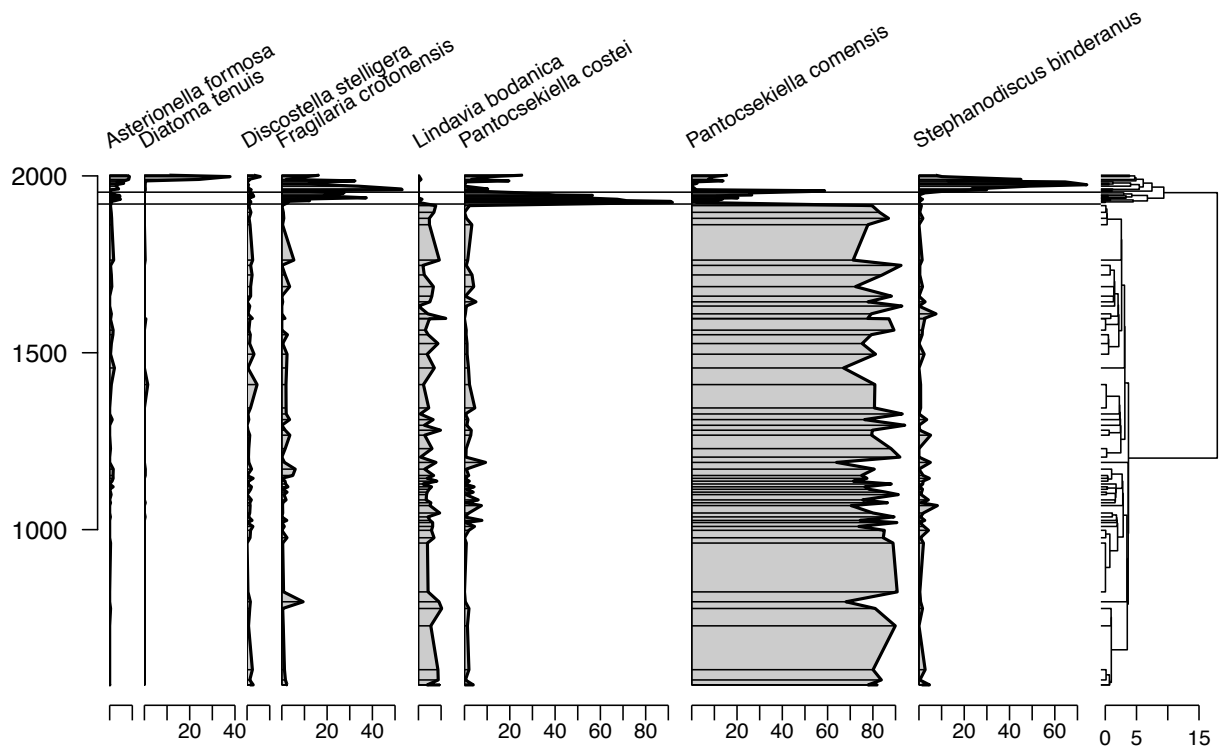
5 **Supplementary Material S2 – Total Phosphorus in Lake Geneva: long-term monitoring**  
6 **data and inference from diatoms assemblages**

7 Lake Geneva total phosphorus concentrations (TP) have been measured once or twice a month  
8 at the deepest point of the lake since 1958 (Système d’Observation et d’Expérimentation au  
9 long terme pour la Recherche en Environnement – Observatoire des Lacs alpins –  
10 <http://www6.dijon.inra.fr/thonon/L-observatoire-OLA>). In the first years of available  
11 monitoring data i.e. from 1958 (first full year), TP concentrations in the epilimnion were around  
12  $12 \mu\text{g TP.L}^{-1}$  but already within an increasing trend confirming that eutrophication had already  
13 started. TP reached  $79 \mu\text{g TP.L}^{-1}$  in 1970, stabilized transiently around  $50 \mu\text{g TP.L}^{-1}$  in the  
14 1972–1986 period, and has been decreasing since then. Current TP concentrations are similar  
15 to those measured during the beginning of the monitoring (close to  $15 \mu\text{g TP.L}^{-1}$ ) (Fig. S2.1).  
16 In order to extend the TP record beyond 1958, total phosphorus concentrations (0-20 m) were  
17 inferred from the composition of subfossil diatoms in LEM10-CC. Previous works on short  
18 cores, covering 1880-2010, had confirmed that diatom-inferred TP provide reliable estimates  
19 in Lake Geneva (Berthon et al. 2013) and capture changes in epilimnetic (0-20m) TP  
20 concentrations above  $8 \mu\text{g.L}^{-1}$ .



21  
 22 **Figure S2.1.** Total phosphorus (TP) in Lake Geneva. Solid green line corresponds to diatom  
 23 inferred TP (DI-TP) from LEM10-CC core. Green envelop depict the interval of confidence  
 24 (95%) of the DI-TP, calculated by bootstrap with 1000 iterations. Black squares are epilimnetic  
 25 TP from long-term monitoring (1958–2015, SOERE OLA). The top-left graph shows the detail  
 26 for the 1940-2015 period.

27  
 28 Diatoms counting were carried out on sub-samples of LEM10-CC. Sub-samples for diatom  
 29 analysis were cleaned with H<sub>2</sub>O<sub>2</sub> and HCl following Renberg (1990). Diatom frustules were  
 30 mounted in Naphrax. On each slide, at least 300 valves were counted and identified by light  
 31 microscopy, using phase contrast with 1000× magnification, following Krammer and Lange-  
 32 Bertalot (1986, 1988, 1991a, b). Description of changes in the diatom assemblage was done  
 33 resorting to stratigraphically constrained hierarchical clustering (CONISS), using R version  
 34 3.1.2 (R Core Team 2014), as well as the *rioja* package (Juggins 2015). Mean total phosphorous  
 35 concentrations were reconstructed from a diatom-based inference model based on 345 surface  
 36 sediment samples collected in lakes in Europe along a trophic gradient  
 37 (<http://craticula.ncl.ac.uk/Eddi>, Battarbee et al. 2001). The calibration dataset covered a large  
 38 trophic gradient, with mean annual TP ranging from 2 to 1189 µgP.L<sup>-1</sup>. Reconstruction was  
 39 performed, using weighted averaging with inverse deshrinking (ter Braak and van Dame 1989).  
 40 The root mean squared error of prediction (RMSEP) was calculated for each sample set using  
 41 bootstrapping with 1000 cycle. Diatom profiles and lake DI-TP reconstruction were performed  
 42 using program C2 (version 1.7.2, Juggins 2007).



43

44 **Figure S2.2.** Summary diatom stratigraphy of the most common taxa in Lake Geneva LEM10-  
 45 CC sequence. The horizontal lines mark the two significant changes in diatom assemblage at  
 46 the scale of the study.

47

48 The paleo-record, on which a hierarchical CONISS analysis was performed, revealed two  
 49 significant changes in the subfossil diatom assemblage of Lake Geneva between 563 and 2010,  
 50 and both took place in the 20<sup>th</sup> century (1916 / 1925 and 1952 / 1956) (Fig. S2.2). Before 1916,  
 51 the assemblage was largely dominated by the centric species *Pantocsekiella comensis* (70-80  
 52 %), seconded by *Lindavia bodanica* (5-10 %), both species typical of oligotrophic waters. The  
 53 subfossil diatom record had been stable for the whole 1400 year-long record (Fig. S2.2). Only  
 54 a slight 8% increase of *Pantocsekiella costei* during the 11<sup>th</sup> century was worth noticing.  
 55 Inferred-TP were thereby stable and low (< 14 µg.L<sup>-1</sup>) before the 20<sup>th</sup> century, typical for an  
 56 oligo/oligomesotrophic lake. From 1925 and up to 1952, *P. comensis* got substituted by  
 57 *Pantocsekiella costei*, another species affiliated to nutrient poor waters. *Fragilaria crotonensis*  
 58 made up to 50% of the assemblage. *F. crotonensis* is somewhat distinctive of waters with higher  
 59 nutrient levels. The increased contribution of *F. crotonensis* could thereby illustrate a slow and  
 60 slight increase in TP as soon as the 1920s. Thereby inferred TP remained below 14 µg.L<sup>-1</sup> for  
 61 this time-period, excluding any important human driven change in TP in the lake before the  
 62 1950s. The second transition in in 1952 / 1956 marked the loss of *Pantocsekiella* sp., while *F.*

63 *crotonensis* declined in favor of *Stephanodiscus binderanus* that represented up to 74% of the  
64 assemblage in 1971. This specific succession is typical for eutrophication and not surprisingly,  
65 inferred TP increased up to 109  $\mu\text{g.L}^{-1}$  in 1979, mirroring measured trends in total phosphorus  
66 concentrations. Not significant at the time-scale of the study, was the recent reorganisation (in  
67 the four-top-most samples of LEM10-CC i.e. reflecting a change in the interval of 1983 / 1986)  
68 with a return of *Pantocsekiella* sp. (< 20% vs. > 70% before 1916), and new species i.e.  
69 *Asterionella formosa* and *Diatoma tenuis*. The most recent part of the record thereby reflected  
70 the recent abatement in water TP. The good coherence between DI-TP and measured TP, as  
71 well as the confidence in the age models, allowed the creation of a composite TP record  
72 (thereafter referred as to inferred TP, I-TP). DI-TP was used up to 1958 and monitoring data  
73 thereafter, avoiding any uncertainties linked to reconstructions.

74 Changes in diatom inferred-TP are considered as representative and indicative of the local  
75 human activities in the lake watershed (Battarbee et al. 2005). Juggins *et al.* (2013) noted that  
76 a number of calibration data sets for diatoms infer secondary gradients and not the major  
77 gradient affecting diatom species composition. Indeed, weighted averaging calibration assumes  
78 that the species respond to an environmental gradient (e.g. [TP]) according to a Gaussian  
79 distribution and that the taxa with an ecological optimal TP close to that of the lake will occur  
80 with greater abundance. However, the calibration used (Battarbee 2000) was mainly based on  
81 the classic trophic sequence from *Pantocsekiella comensis* to *Asterionella/Fragilaria*  
82 *crotonensis* to *Stephanodiscus* (Harris 1987), which reflects the known ecology of the main  
83 planktonic diatoms (Willen 1991; Hall and Smol 2010) and was, therefore, considered reliable  
84 (Juggins 2013, p384). The reliability of the diatom inferences based on this sequence has been  
85 shown in the present study and elsewhere by comparing the DI-TP with historical TP values  
86 (e.g. Marchetto and Bettinetti 1995). However, because a small lag in diatoms responses in  
87 Lake Geneva has been documented, we used a composite TP record (DI-TP until 1957,  
88 monitoring data from 1958), thereafter referred to as I-TP. The confidence in I-TP is very high  
89 as the first changes in diatoms communities took place at the beginning of the monitoring  
90 program.

91

## 92 **References**

93 Battarbee RW (2000) Palaeolimnological approaches to climate change, with special regard to  
94 the biological record. *Quat Res* 19:107–124

- 95 Battarbee RW, John Anderson N, Jeppesen E, Leavitt PR (2005) Combining  
 96 palaeolimnological and limnological approaches in assessing lake ecosystem response  
 97 to nutrient reduction. *Freshw Biol* 50:1772–1780. [https://doi.org/10.1111/j.1365-](https://doi.org/10.1111/j.1365-2427.2005.01427.x)  
 98 2427.2005.01427.x
- 99 Battarbee RW, Juggins S, Gasse F, et al (2001) European diatom database (EDDI). An  
 100 information system for palaeoenvironmental reconstruction. University College,  
 101 London
- 102 Berthon V, Marchetto A, Rimet F, et al (2013) Trophic history of French sub-alpine lakes over  
 103 the last ~150 years: phosphorus reconstruction and assessment of taphonomic biases. *J*  
 104 *Limnol* 72:34. <https://doi.org/10.4081/jlimnol.2013.e34>
- 105 Hall RI, Smol JP (2010) Diatoms as indicators of lake eutrophication. In: *The Diatoms:*  
 106 *Applications for the Environmental and Earth Sciences* 2nd edition, Cambridge  
 107 University Press. Smol, J.P. & Stoermer, E.F., Cambridge, pp 122–151
- 108 Harris GP (1987) *Phytoplankton Ecology*. Springer Netherlands, Dordrecht
- 109 Juggins S (2015) rioja: Analysis of Quaternary Science Data, R package version (0.9-5)
- 110 Juggins S (2007) C2 Version 1.7 User guide. Software for ecological and palaeoecological data  
 111 analysis and visualisation. Newcastle upon Tyne, UK
- 112 Juggins S (2013) Quantitative reconstructions in palaeolimnology: new paradigm or sick  
 113 science? *Quaternary Science Reviews* 64:20–32.  
 114 <https://doi.org/10.1016/j.quascirev.2012.12.014>
- 115 Krammer K, Lange-Bertalot H (1991a) *Bacillariophyceae*. 3. Teil: Centrales, Fragilariaceae,  
 116 Eunotiaceae, Gustav Fischer Verlag. Ettl, H., Gerloff, J., Heynig, H. and Mollenhauer,  
 117 D., Stuttgart, Jena
- 118 Krammer K, Lange-Bertalot H (1991b) *Bacillariophyceae*. 4. Teil: Achnanthaceae, Kritische  
 119 Ergänzungen zu *Navicula* (Lineolatae) und *Gomphonema*, Gesamtliteraturverzeichnis,  
 120 Gustav Fischer Verlag. Ettl, H., Gerloff, J., Heynig, H. and Mollenhauer, D., Stuttgart,  
 121 Jena
- 122 Krammer K, Lange-Bertalot H (1988) *Bacillariophyceae*. 2. Teil: Bacillariaceae,  
 123 Epithemiaceae, Surirellaceae, Gustav Fischer Verlag. Ettl, H., Gerloff, J., Heynig, H.  
 124 and Mollenhauer, D., Jena
- 125 Krammer K, Lange-Bertalot H (1986) *Bacillariophyceae*. 1. Teil: Naviculaceae, Gustav Fischer  
 126 Verlag. Ettl, H., Gerloff, J., Heynig, H. and Mollenhauer, D., Stuttgart, New York.
- 127 Marchetto A, Bettinetti R (1995) Reconstruction of the phosphorus history of two deep,  
 128 subalpine Italian lakes from sedimentary diatoms, compared with long-term chemical  
 129 measurements. *Memorie dell’Istituto Italiano di Idrobiologia “Dott Marco De Marchi”*  
 130 53:27–38
- 131 R Core Team (2014) *R: A language and environment for statistical computing*. R Foundation  
 132 for Statistical Computing, Vienna, Austria

- 133 Renberg I (1990) A procedure for preparing large sets of diatom slides from sediment cores. J  
134 Paleolimnol 4:87–90
- 135 ter Braak CJF, van Dame H (1989) Inferring pH from diatoms: a comparison of old and new  
136 calibration methods. Hydrobiologia 178:209–223. <https://doi.org/10.1007/BF00006028>
- 137 Willen E (1991) Planktonic diatoms - an ecological review. Algological Studies 62:69–106
- 138